Journal of
Instrumentation

PAPER • OPEN ACCESS

High-level hadronic tau lepton triggers of the CMS experiment in proton-proton collisions at √(s) = 13.6 TeV

To cite this article: A. Hayrapetyan *et al* 2026 *JINST* **21** P04002

Jinst

Published by IOP Publishing for Sissa Medialab

Received: *February 11, 2026*
Accepted: *February 18, 2026*
Published: *April 2, 2026*

High-level hadronic tau lepton triggers of the CMS experiment in proton-proton collisions at $\sqrt{s} = 13.6$ TeV

The CMS collaboration

Full author list at the end of the paper

E-mail: cms-publication-committee-chair@cern.ch

Abstract: The trigger system of the CMS detector is pivotal in the acquisition of data for physics measurements and searches. Studies of final states characterized by hadronic decays of tau leptons require the reconstruction and the identification of genuine tau leptons against quark- and gluon-initiated jets at the trigger level. This is a difficult task, particularly as improvements to the LHC have resulted in an increased number of interactions per bunch crossing in recent years. To address this challenge, a series of machine-learning algorithms with high identification efficiency and low computational cost have been incorporated into the high-level trigger for hadronically decaying tau leptons. In this paper, these developments and the trigger performance are summarized using data collected by the CMS experiment in proton-proton collisions at $\sqrt{s} = 13.6$ TeV in 2022–2023, corresponding to an integrated luminosity of $62\,\text{fb}^{-1}$.

Keywords: Particle identification methods; Trigger detectors

https://doi.org/10.1088/1748-0221/21/04/P04002

Contents

1 Introduction

The tau lepton (τ) is widely used in measurements and searches carried out using proton-proton (pp) collision data recorded at the CERN LHC. The tau lepton's importance is most apparent in the observation and the measurements of the standard model (SM) Higgs boson decaying to a pair of tau leptons [1–7], the precision measurements of the tau lepton anomalous magnetic moment [8, 9], and the measurements of the tau lepton polarization [10–12]. Moreover, final states including tau leptons are at the forefront of searches for beyond-the-SM (BSM) particles, processes, and couplings [13, 14].

Tau leptons are massive enough to decay hadronically, and are the heaviest leptons in the SM, possessing a mass of 1.777 GeV and mean lifetime of 290 fs [15]. Because of the short lifetime, tau leptons produced by pp collisions in CMS are not detected directly and can only be reconstructed from their decay products. Tau leptons decay hadronically with a branching fraction of 64.8%, resulting in one tau neutrino (ν_τ) and two quarks. The quarks undergo hadronization, and the final object is reconstructed as a hadronic tau (τ_h) candidate. The remaining branching fraction comprises leptonic decays, either to an electron or a muon, and accompanying neutrinos.

2026 JINST 21 P04002

In this paper, we describe for the first time the developments of machine-learning (ML) algorithms deployed into the high-level trigger (HLT) in the CMS experiment [16, 17] for identifying τ_h candidates. The performance is evaluated using pp collision data collected in 2022–2023 at a center-of-mass energy of 13.6 TeV, which we refer to as "early Run 3" or simply "Run 3" throughout the paper. Similarly, we use "Run 2" to refer to the data-taking period from 2016–2018. Run 3 is the first time that the HLT is equipped with ML algorithms for τ_h candidates. Because of these advancements and the instrumental upgrades [17], the HLT τ_h candidates are captured with higher efficiency than in Run 2 [18], despite an aging detector and an increased number of additional pp interactions per bunch crossing.

This paper is structured as follows: section 2 introduces the CMS detector with emphasis on its two-tiered trigger system, followed by a description of the offline event reconstruction in section 3. Sections 4 and 5 describe the samples used for HLT development and performance evaluation, and τ_h candidate reconstruction at the HLT, respectively. Sections 6 and 7 focus on the development of ML algorithms for τ_h candidate identification at the HLT. Section 8 discusses the performance of τ_h candidate reconstruction in early Run 3 data, and a summary is given in section 9.

2 The CMS detector

The CMS apparatus [16, 17] is a multipurpose, nearly hermetic detector, designed to trigger on [19–21] and identify electrons, muons, photons, and (charged and neutral) hadrons [22–24]. Its central feature is a superconducting solenoid of 6 m internal diameter, providing a magnetic field of 3.8 T. A silicon pixel and strip tracker, a lead tungstate crystal electromagnetic calorimeter (ECAL) with silicon strip preshower detectors placed at the front faces of the two endcap calorimeters, and a brass and scintillator hadron calorimeter (HCAL), each composed of a barrel and two endcap sections, are installed inside the solenoid. Forward calorimeters extend the pseudorapidity (η) coverage provided by the barrel and endcap detectors. Muons are detected in gas-ionization chambers embedded in the steel flux-return yoke outside the solenoid. A more detailed description of the CMS detector, together with a definition of the coordinate system and the relevant kinematic variables, is presented in refs. [16, 17].

Before the start of the 2022 data-taking period, numerous upgrades and improvements to the subdetectors, readout electronics, trigger, data acquisition, software, and offline computing systems were implemented. These include new silicon photomultipliers and readout electronics for the HCAL that allow for a finer granularity and longitudinal segmentation [25], the replacement of the innermost layer of the silicon pixel detector [26], the new hybrid CPU/GPU farm for the HLT [27], and the rebuilt dedicated online luminosity monitors [28–30].

Events of interest are selected using a two-tiered trigger system. The first level (L1), composed of custom hardware processors, uses information from the calorimeters and muon detectors to select events at a rate of around 100 kHz within a fixed latency of 4 μs [19]. The second level, known as the HLT, consists of a farm of processors running a version of the full event reconstruction software optimized for fast processing, and reduces the event rate to a few kHz before data storage [20, 21]. An HLT "path" is a sequence of algorithms and selections that performs a simplified event reconstruction during data taking and targets a physics process. In Run 3, the full HLT menu consists of about 800 different HLT paths [20]. The term "online" is used to refer to quantities calculated and physics objects produced at the time of data taking, to determine if an event will be stored for later analysis. If an event is accepted by the HLT based on its online information, a more sophisticated "offline" reconstruction is performed and used for further analysis.

2026 JINST 21 P04002

3 Reconstruction of offline objects

This section describes the general reconstruction methods of physics objects used in the training and performance evaluation for offline studies.

Final-state particles, such as electrons, muons, and charged and neutral hadrons, are reconstructed by the particle-flow (PF) algorithm [31], which uses an optimized combination of information from subdetectors of the CMS experiment. The energy of photons is obtained from the ECAL measurement. The energy of electrons is determined from a combination of the electron momentum at the primary interaction vertex from the tracker, the energy of the corresponding ECAL cluster, and the energy sum of all bremsstrahlung photons spatially compatible with originating from the electron track. The momentum of muons is obtained from the curvature of the corresponding track. The energy of charged hadrons is determined from a combination of their momentum measured in the tracker and the matching ECAL and HCAL energy deposits, corrected for the response function of the calorimeters to hadronic showers. Finally, the energy of neutral hadrons is obtained from the corresponding corrected ECAL and HCAL energies. These particles are then used to reconstruct higher-level physics objects, including jets, missing transverse momentum, and τ_h candidates. The primary vertex is taken to be the vertex corresponding to the hardest scattering in the event, evaluated using tracking information alone, as described in ref. [32].

For each event, hadronic jets are clustered from these reconstructed particles using the infrared and collinear safe anti-k_T algorithm [33, 34] with a distance parameter of 0.4. The jet momentum is determined as the vectorial sum of all particle momenta in the jet, and is found from simulation to be, on average, within 5 to 10% of the generator-level momentum over the whole transverse momentum (p_T) spectrum and detector acceptance. Additional pp interactions within the same or nearby bunch crossings (pileup) can contribute additional tracks and calorimetric energy depositions to the jet momentum. To mitigate this effect, charged particles identified to be originating from pileup vertices are discarded and an area-based offset correction is applied during Run 2 [35], whereas the pileup-per-particle identification algorithm is used during Run 3 [36]. Jet energy corrections are derived from simulation to bring the measured response of jets to that of particle level jets on average. In situ measurements of the momentum balance in dijet, photon+jet, Z+jet, and multijet events are used to account for any residual differences in the jet energy scale between data and simulation [37]. The jet energy resolution amounts typically to 15–20% at 30 GeV, 10% at 100 GeV, and 5% at 1 TeV [37]. Additional selection criteria are applied to each jet to remove jets potentially dominated by anomalous contributions from various subdetector components or reconstruction failures [35].

Electrons are measured in the range $|\eta| < 2.5$. The reconstruction efficiency in data ranges from 88 to 98% in the barrel region ($|\eta| < 1.479$) and from 90 to 96% in the endcaps ($1.479 < |\eta| < 2.5$) for electrons in the p_T range between 10 and 100 GeV. The momentum resolution for electrons with $p_T \approx 45$ GeV from $Z \to ee$ decays ranges from 1.7 to 4.5%. It is generally better in the barrel region than in the endcaps, and also depends on the bremsstrahlung energy emitted by the electron as it traverses the tracker material before reaching the ECAL [38].

Muons are measured in the range $|\eta| < 2.4$, with detection planes made using three technologies: drift tubes, cathode strip chambers, and resistive plate chambers. The single muon trigger efficiency exceeds 90% over the full η range, and the efficiency to reconstruct and identify muons is greater than 96%. Matching muons to tracks measured in the silicon tracker results in a relative p_T resolution of 1% in the barrel and 3% in the endcaps for muons with $p_T < 100$ GeV. Measurements made

2026 JINST 21 P04002

with cosmic ray muons show that, in the central region of the detector, the p_T resolution is better than 7% for muons with p_T up to 1 TeV [23].

The missing transverse momentum vector, $\vec{p}_T^{\,miss}$, is computed as the negative vectorial sum of all the PF candidate p_T in an event, and its magnitude is denoted as p_T^{miss} [39]. The $\vec{p}_T^{\,miss}$ is modified to include corrections to the energy scale of the reconstructed jets in the event.

Jets are used as seeds in the reconstruction of τ_h candidates, which is carried out with the hadron-plus-strips (HPS) algorithm [18, 40, 41], analogously to the logic in the HLT described in section 5. To distinguish genuine τ_h decays from jets originating from the hadronization of quarks or gluons, and from electrons or muons, the DeepTau algorithm is used [42, 43], and its online implementation is discussed in detail in section 7.

4 Data and simulated samples

The early Run 3 data collected by the CMS detector correspond to 34.7 (27.2) fb^{-1} of pp collisions from 2022 (2023) [44–47]. Further event selection criteria are applied depending on the analyses performed and are described in detail in the relevant sections.

Monte Carlo (MC) samples are produced for ML algorithm training and trigger performance evaluation. Drell-Yan (DY) ($Z/\gamma^* \to \ell\ell$, where $\ell = e, \mu, \tau$) and W+jet samples of simulated events are produced at leading order (LO) using MadGraph5_amc@nlo 2.6.5 [48] with the MLM jet merging scheme [49]. Events comprised predominantly of jets produced through the strong interaction, referred to as quantum chromodynamic (QCD) multijet events, are simulated at LO with pythia 8.243 [50]. Top quark-antiquark pairs ($t\bar{t}$) are simulated at next-to-LO with powheg v2 [51–55]; this generator is also used for Higgs boson production via vector boson fusion at next-to-LO [56] followed by the Higgs boson decaying to two tau leptons ($H \to \tau\tau$). The pythia generators are used together to produce a BSM sample of a heavy gauge boson decaying to two tau leptons ($Z' \to \tau\tau$), where the Z' boson mass is 4 TeV. The pythia generator, with the CP5 underlying-event tune [57], is interfaced with the matrix-element generators to model tau lepton decays by tauola [58], the parton shower, and hadronization processes. The NNPDF 3.0 or 3.1 parton distribution functions are used as input in all the calculations [59, 60]. For all MC samples, the detector response is simulated using a detailed description of the CMS detector based on Geant4 [61], and event reconstruction is performed on simulation with the same algorithms as are used for data.

The simulated events are reweighted with the same pileup profile as found in the observed data. In 2022 and 2023, the average number of interactions per bunch crossing was 46 and 52, respectively [44].

5 Reconstruction of τ_h candidates at the HLT

5.1 Tau trigger reconstruction

The tau lepton decay branching fractions are summarized in table 1. As described in the introduction, the tau lepton can decay leptonically or hadronically. The key property of hadronic tau lepton decays is that they primarily proceed through mesonic resonances via an electroweak charged current interaction. These hadronic decay products provide characteristic information to reconstruct and identify tau leptons in an event.

All HLT paths begin with, or are "seeded" by, an L1 trigger. The L1 τ_h candidate algorithm begins by identifying locally maximal energy deposits above a threshold of 2 GeV. Using only position and

2026 JINST 21 P04002

Table 1. Decay modes and branching fractions ($\mathcal{B}$) of the tau lepton alongside the mesonic resonances primarily involved in hadronic tau lepton decays. Reproduced from [15]. CC BY 4.0.

Decay mode		$\mathcal{B}$ [%]	Resonance [MeV]
Leptonic decays	35.2		
$\tau^- \to e^- \overline{\nu}_e \nu_\tau$		17.8	
$\tau^- \to \mu^- \overline{\nu}_\mu \nu_\tau$		17.4	
Hadronic decays	64.8		
$\tau^- \to h^- \nu_\tau$		11.5	
$\tau^- \to h^- \pi^0 \nu_\tau$		26.0	$\rho(770)$
$\tau^- \to h^- \pi^0 \pi^0 \nu_\tau$		9.5	$a_1(1260)$
$\tau^- \to h^- h^- h^+ \nu_\tau$		9.8	$a_1(1260)$
$\tau^- \to h^- h^- h^+ \pi^0 \nu_\tau$		4.8	
Other hadronic modes		3.2	

energy information from the ECAL and HCAL, the algorithm builds clusters and merges them based on proximity conditions determined by the size of ECAL and HCAL detector elements, and the position of the local maxima in η. Then, the τ_h candidate's position is computed as an energy-weighted average centered around the largest energy deposit. This is an effective first step to identify τ_h candidates because hadronically decaying tau leptons typically have less hadronic activity than QCD-induced jets, leading to a smaller total size and fewer clusters of energy deposition. Isolation requirements to suppress the surrounding energy deposit are applied as a function of the τ_h candidate's total energy, η, and the number of calorimeter trigger towers (n_{TT}) in order to suppress the QCD-induced jets, which are usually broader. Calorimeter trigger towers group 5×5 ECAL crystals in the barrel and the corresponding HCAL tower behind them into one object with a total size of $\Delta\eta\times\Delta\phi = 0.087\times0.087$, where ϕ is the azimuthal angle in radians. The isolation requirements are loosened for high n_{TT} and high total energy to minimize the efficiency dependence on pileup and maximize the efficiency. A full description of all L1 trigger objects and algorithms is given in ref. [19]. The efficiency of both isolated and nonisolated τ_h candidates from L1 is typically greater than 80% for 10 GeV above its threshold value and greater than 90% for 20 GeV above it [62].

The HLT is designed to use fast and simple algorithms to quickly reject lower quality events before running more complex reconstruction on passing events. Consequently, the τ_h candidate reconstruction at the HLT is performed in several steps depending on the final state targeted by the path, which includes di-τ_h, single-τ_h, eτ_h, and $\mu\tau_h$. A brief overview of the Run 2 τ_h candidate reconstruction steps at the HLT, discussed extensively in ref. [21], is given first to contrast the updated Run 3 approach.

In Run 2, the online workflow begins with L1 τ_h objects as seeds, and, depending on the HLT path, is then followed by so-called L2, L2.5, and L3 steps, which are progressively more complex. A diagram of the workflow is shown in figure 1, as some HLT paths only need to run a subset of these steps. The so-called cross trigger eτ_h and $\mu\tau_h$ HLT paths already have low event rates due to the light-lepton reconstruction and identification, hence the L2 and L2.5 filtering steps are not necessary. For the single-τ_h and di-τ_h HLT paths, the L2 step combines L1 information with energy deposition information in the calorimeter towers, then the L2.5 step uses additional information from the pixel detector to compute a charged-particle isolation score. Finally, if the τ_h candidates pass the

2026 JINST 21 P04002

previous steps, they proceed to the L3 step, where online PF reconstruction is performed using the full tracking information. All paths except the di-τ_h one adopt a global reconstruction of all tracks in the event. The di-τ_h path applies a regional reconstruction with tracks localized around the L2 τ_h candidate. The algorithms used in Run 2 paths are referred to as "cut-based" algorithms because they enforce threshold values on relatively simple observables.

In Run 3, the overall workflow is the same, but the cut-based algorithms previously used at the L2 and L3 steps have been replaced with ML algorithms, as shown in red in figure 2. These updates include a convolutional neural network based algorithm at the L2 step, called L2TauNNTag, that was developed to suppress the event rate to an affordable value in single-τ_h and di-τ_h HLT paths, as discussed in detail in section 6. The updated L3 reconstruction step adopts online τ_h candidate identification using a simplified version of the DeepTau network, as discussed in section 7.

The eτ_h and $\mu\tau_h$ cross triggers are designed to capture events with one τ_h candidate in association with an electron or muon. The eτ_h HLT path is seeded with an electromagnetic object and a τ_h candidate from the L1 trigger. The electromagnetic object can be an electron or photon, and is required to have $p_T > 22$ GeV and satisfy a loose isolation criterion, determined by the number of hits in nearby trigger towers as a function of p_T. The L1 τ_h candidate is required to have $p_T > 26$ GeV and satisfy similarly defined isolation criteria. The objects are required to not overlap within a cone of $\Delta R = \sqrt{(\Delta\eta)^2 + (\Delta\phi)^2} < 0.3$. The $\mu\tau_h$ HLT path is seeded with an L1 muon object with $p_T > 18$ GeV and an L1 τ_h candidate with $p_T > 24$ GeV. No isolation is required in the case of the $\mu\tau_h$ L1 trigger. At HLT, the electron (muon) is required to have $p_T > 24$ (20) GeV and satisfy tight identification and isolation criteria, which reduces the rate of events for the τ_h candidate reconstruction.

The L3 τ_h candidate reconstruction uses the full tracking information with the online PF reconstruction, and is a simplified version of the offline algorithm [31] in order to reduce the processing time. With these inputs, a simplified version of the HPS algorithm is applied, modified from the offline τ_h candidate reconstruction, and discussed extensively in ref. [18]. More details of the online HPS algorithm are given in section 5.2. The tau lepton identification (tau-ID) score of the reconstructed τ_h candidate is computed with the online version of DeepTau. Finally, the τ_h candidate is required to have $p_T > 30$ (27) GeV for the eτ_h ($\mu\tau_h$) HLT path, and not overlap with the light lepton within a cone of $\Delta R < 0.5$.

The single-τ_h HLT path is designed to capture events with at least one high-p_T τ_h candidate. The HLT path is seeded with a τ_h candidate from L1 with $p_T > 120$ GeV, and no isolation requirement. The single-τ_h HLT path makes use of the L2TauNNTag algorithm to reduce the rate of events entering the final L3 reconstruction. The previously described L3 reconstruction is then followed by the online tau-ID with DeepTau, and finally a requirement that the τ_h candidate has $p_T > 180$ GeV.

The di-τ_h HLT path is meant to capture events with at least two τ_h candidates. It is seeded by two isolated L1 τ_h candidates, each with $p_T > 32$ GeV. This threshold was increased to 34 GeV in the later portion of 2022 data taking to mitigate a larger-than-expected L1 rate. If there are two L1 τ_h candidates with $p_T > 70$ GeV, no isolation criteria are applied. Similar to the single-τ_h HLT path, the L2TauNNTag is used to reduce the input rate to the next reconstruction step. Again, the L3 reconstruction is performed, an online tau-ID score is evaluated with DeepTau, and a p_T threshold of 35 GeV is applied to both τ_h candidates. Additionally, the candidates are required to not overlap within a cone of $\Delta R < 0.5$.

2026 JINST 21 P04002

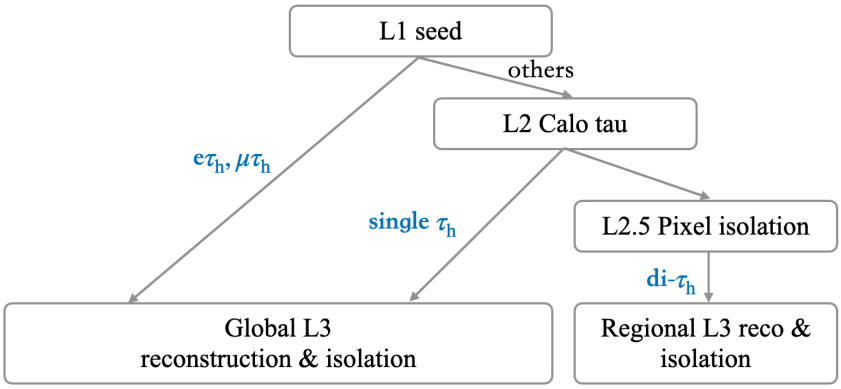

Figure 1. Workflows for τ_h candidate reconstruction at the HLT in Run 2. Reproduced from [21]. The Author(s). CC BY 4.0.

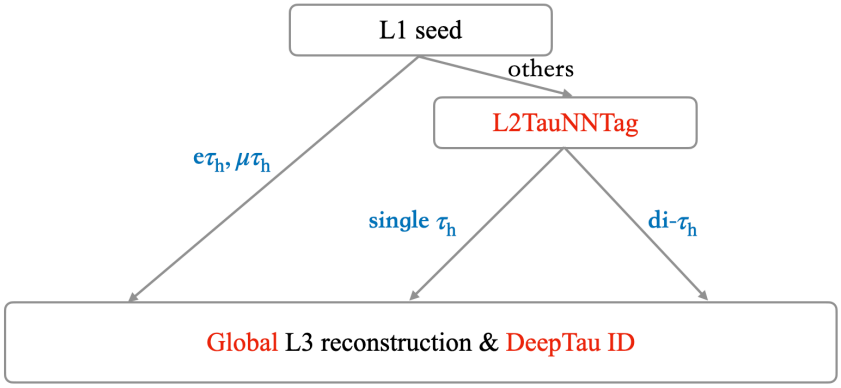

Figure 2. Workflows for τ_h candidate reconstruction at the HLT in Run 3, since 2022.

5.2 The HPS algorithm

The HPS algorithm was first used for the offline reconstruction of hadronic tau lepton decays in Run 2 [18, 40, 41]. It was then introduced online to HLT paths with τ_h candidates in 2018 to replace the cone-based algorithm [18]. The initial inputs to the algorithm are PF jets with $p_T > 14$ GeV and $|\eta| < 2.5$ that were reconstructed using the anti-k_T algorithm with a distance parameter of $R = 0.4$ [31].

Targeting the hadronic decay modes in table 1, the algorithm reconstructs τ_h candidates using the features of charged hadrons and neutral pions. The neutral pions rapidly decay into photon pairs, a fraction of which can interact with the nuclei and associated electrons in the tracker material leading to photon conversion into e^+e^- pairs. The strong magnetic field of the CMS detector's solenoid bends the pair of e^+ and e^- into opposite directions in ϕ, resulting in a spatial separation in the η–ϕ plane. Photon and electron candidates that are found in the online PF jets are clustered into a "strip" with a $\Delta\eta\times\Delta\phi$ area of 0.05×0.2 around the highest p_T photon or electron. The wider spread of electrons in the ϕ direction is caused by the CMS experiment's solenoid. The momentum of the strip is defined as the vectorial sum of the momentum of its constituents, and the mass is assigned to be the π^0 mass. Only the strips with $p_T > 2.5$ GeV are considered.

The cone size for reconstructing a τ_h candidate is defined as $R_{sig} = 3\,\text{GeV}/p_T$, with the limits of $0.05 < R_{sig} < 0.10$, where p_T is that of the hadronic system. All strips and charged hadrons in

2026 JINST 21 P04002

the cone are used to reconstruct the τ_h candidate. It is possible to construct multiple τ_h candidates for a single jet, in which case the one with the largest p_T is selected.

The number of charged and neutral hadrons, $N_{h^\pm}$ and N_{π^0}, are used to classify the reconstructed τ_h candidates. For each charged hadron, there is a distinguishable track, and the decay modes are subsequently grouped into "*n-prong*" (the number of charged hadrons) cases. For 3-prong decay modes, the summed charge of the constituents is required to equal ±1. Since the 2-prong cases violate charge conservation, they are considered to be 3-prong decays where one charged hadron was misreconstructed or escaped the detector acceptance. Further requirements of matching with the resonances listed in table 1 are realized by constraining the invariant mass of charged and neutral particles to the mass windows of $\rho(770)$ or $a_1(1260)$, optimized under dedicated online conditions.

6 The L2TauNNTag algorithm at the HLT

In Run 3, the cut-based L2 and L2.5 sequences from Run 2 have been replaced by a convolutional neural network, L2TauNNTag, described here for the first time. This new algorithm adopts ML to accommodate more available information in order to improve the efficiency of genuine τ_h candidates in τ_h HLT paths, while lowering or maintaining the rate budget with respect to Run 2. However, the event rates in τ_h HLT paths are still dominated by background from QCD jets. The algorithm takes advantage of new GPU-based tracks from the pixel detector [63, 64] in addition to the calorimeter information. Its training is performed on τ-enriched MC samples of DY, $t\bar{t}$, and W+jet for genuine hadronic tau lepton decays, as well as QCD events for jets misidentified as hadronic tau lepton decays. The generator-level p_T distribution of each sample is reweighted to obtain a uniform yield in each bin.

6.1 Network architecture

There are several types of input features used in the L2TauNNTag, which will be listed in increasing order of granularity. At the global level of an event, the number of vertices is reconstructed using Patatracks, a set of GPU-based software developed for optimizing and accelerating data processing for pixel track reconstruction in the HLT and offline computing [63, 64]. At the object level, the properties of L1 τ_h candidates are used, including p_T, η, ϕ, and isolation. Further down to the detector level, the energy deposit information in the ECAL and HCAL linked to the L1 τ_h candidates is also used, consisting of the total energy detected, the number of energy deposits, the distances in η and ϕ between these deposits and the τ_h candidate, a chi-squared (χ^2) value assessing the consistency of the detected energy with respect to the expected pattern of genuine tau leptons, as well as the total energy sum and energy deposit multiplicity for cases with nonzero χ^2 values. In addition to the calorimeter information, the Patatrack observables for each L1 τ_h candidate are used, including the number of associated tracks and the scalar sum of their p_T, a flag indicating the presence of an associated reconstructed vertex, the charge associated with the tracks, the η and ϕ distance between the tracks and the L1 τ_h candidate, the χ^2 and number of degrees of freedom of the track reconstruction, as well as the longitudinal (d_z) and transverse impact parameters.

To structure the data, the input features are organized in a 5×5 grid in the η–ϕ plane, and are connected to four convolution layers with a 1×1 window (numbers of filters are 80, 60, 40, and 20), followed by four convolution layers with a 2×2 window (numbers of filters are 20, 20, 20, and 40). These are then interfaced to three dense layers (numbers of nodes are 40, 40, and 20) and a final dense layer with a sigmoid function. Batch normalization and the rectified linear unit activation function are

2026 JINST 21 P04002

used in each layer before the final layer. The loss function used is binary cross entropy, and the total number of trainable parameters is 23 701. The training procedure employs the Adam optimizer [65] with a learning rate of 0.001. Once the validation loss reaches its minimum value, the model parameters are stored. An early stopping criteria is applied, such that the training is terminated if the validation loss does not exhibit any improvement for ten consecutive epochs. The dataset is partitioned into three subsets, using 60% of the total dataset for training, 20% for testing, and 20% for validation.

6.2 Performance of the L2TauNNTag algorithm

To compare the computing performance of the L2TauNNTag algorithm and the previous L2+L2.5 cut-based approach, the processing time and event rates were evaluated on a machine purpose-built to emulate the real conditions of the HLT computing farm. Three different datasets were used and linearly scaled by instantaneous luminosity to compare event rates from the cut-based and L2TauNNTag algorithms, including Run 2 data, Run 2 data re-emulated under Run 3 trigger conditions, and Run 3 data, as described in table 2. In the di-τ_h HLT path, the L2TauNNTag step results in reduced event rate to the next step of the HLT, with a similar processing time and improved efficiency compared to the L2+L2.5 cut-based approach.

Table 2. Rate estimation and observation for the cut-based and L2TauNNTag algorithms. Column A scales Run 2 data collected by the cut-based algorithm to Run 3 conditions, column B re-emulates Run 2 data using the L2TauNNTag algorithm and scales the result to Run 3 conditions, and column C is the evaluated rate in Run 3. The instantaneous luminosities used were 1.68, 2.00, and $2.20 \times 10^{34}\,\mathrm{cm}^{-2}\,\mathrm{s}^{-1}$, respectively. The rates are inclusive calculations not excluding shared contributions from other algorithms or paths. The statistical uncertainties are negligible with respect to the significant digits reported.

Path	A [kHz]	B [kHz]	C [kHz]
Di-τ_h	6.1	5.4	5.5
Single-τ_h	2.0	1.9	1.4

The efficiency of selecting genuine hadronic tau leptons using the di-τ_h HLT path is compared between the L2+L2.5 cut-based and L2TauNNTag algorithms in figure 3, using simulated $H \to \tau\tau$ and BSM $Z' \to \tau\tau$ events which were not used in the training. The mixture of events from these two processes provides a sufficient sample size in a wide p_T range. The absolute efficiency is calculated using the p_T-leading τ_h candidate and contains both the L1 and L2 steps, accounting for the trigger efficiency. In the left plot, the absolute efficiency of the L2TauNNTag surpasses the L2+L2.5 cut-based approach in almost the full range of visible generator-level τ_h p_T, where "visible" refers to the fact that the contribution of neutrinos is not taken into account. The efficiency jump at 300 GeV is due to a threshold selection, above which all candidates are accepted. This originates from the fact that the L1 τ_h p_T value saturates above 250 GeV due to hardware constraints and is used as an input to the L2TauNNTag. Although the absolute efficiency of the L2+L2.5 cut-based approach is slightly higher than L2TauNNTag in the high-η region, an improvement in efficiency from the L2TauNNTag can be seen in the central region of the visible generator-level η, which most electroweak and targeted BSM physics processes favor. The efficiency reduction in the high-η region is due to the low number of events available in the training samples in that region. Overall, the L2TauNNTag results in better performance for the di-τ_h HLT path than the L2+L2.5 cut-based approach.

2026 JINST 21 P04002

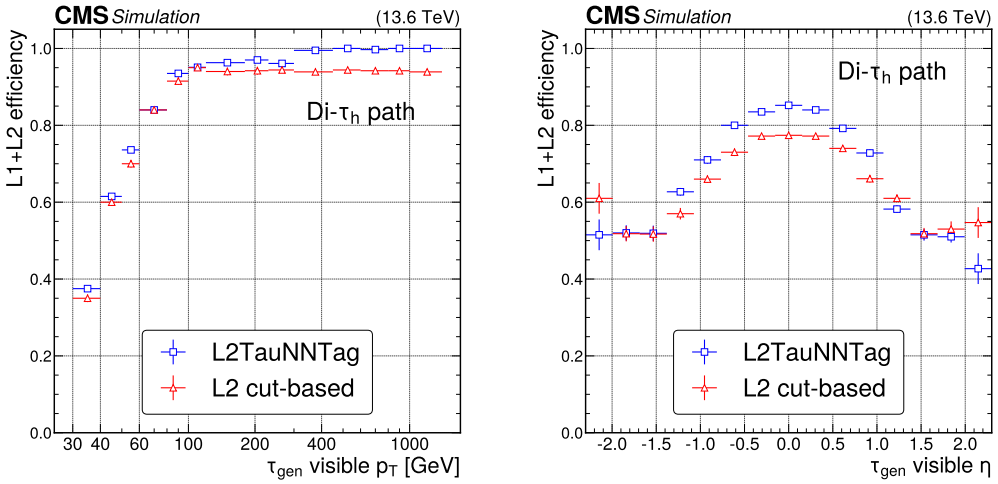

Figure 3. Performance of the L2TauNNTag in the di-τ_h HLT path, using simulated $H \to \tau\tau$ and BSM $Z' \to \tau\tau$ events. The absolute efficiency of the reconstructed L2 τ_h candidates as a function of the visible generator-level τ_h p_T (left) and η (right) are shown, where "visible" refers to the fact that the contribution of neutrinos is not taken into account. The uncertainties shown by the vertical bars are from the number of events available in the sample, while the horizontal bars show the bin width. Some of the vertical bars are smaller than the markers and are not shown.

A comparison between the L2TauNNTag and the L2 cut-based approach is also performed for the single-τ_h HLT path, using simulated $H \to \tau\tau$ and BSM $Z' \to \tau\tau$ events that were not used in the training. The introduction of the L2TauNNTag step reduces the event processing time by roughly 40%, while keeping the event rate unchanged with respect to the previous L2 cut-based approach.

The efficiency of the single-τ_h HLT path is compared between the L2 cut-based and L2TauNNTag algorithms in figure 4. The reduced efficiency in the high-p_T region of the left plot is caused by an L1-to-HLT ΔR-matching requirement, which can fail at high p_T when multiple τ_h candidates are present but only one is reconstructed by either the L1 or HLT. Subsequently, L1-to-HLT matching is not required in the path itself, and the reduced efficiency is understood as an artifact of the selection. Given the high efficiency already obtained in the L2 cut-based approach, the L2TauNNTag was introduced in the single-τ_h path to reduce the processing time while keeping the efficiencies and rates at a similar level.

While both the di-τ_h and single-τ_h HLT paths have been updated to use the L2TauNNTag, the paths have different requirements. In the di-τ_h HLT path, two τ_h candidates are required to pass a neural network discriminant value which was optimized for maximum efficiency improvement. In the single-τ_h HLT path, only one τ_h candidate is required, and it must pass a tighter discriminant value to retain the established efficiency. The differences in efficiency between these two HLT paths are due to these differing object requirements, as displayed in figures 3 and 4.

7 DeepTau implementation in the HLT

The DeepTau algorithm is a multiclass τ_h candidate identification algorithm based on a convolutional deep neural network, originally designed for use on offline objects [66]. The primary goal of DeepTau is to effectively discriminate hadronic tau lepton decays from all three main backgrounds: quark or gluon jets, electrons, and muons. To accomplish this, it is used on PF jets after they have undergone

2026 JINST 21 P04002

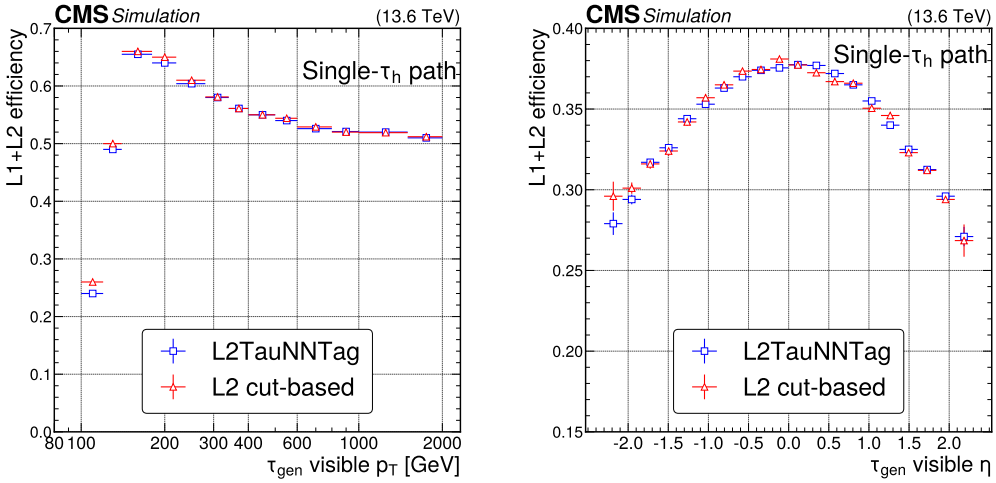

Figure 4. Performance of the L2TauNNTag in the single-τ_h HLT path, using simulated $H \to \tau\tau$ and BSM $Z' \to \tau\tau$ events. The absolute efficiency of the reconstructed L2 τ_h candidates as a function of the visible generator-level τ_h p_T (left) and η (right) are shown, where "visible" refers to the fact that the contribution of neutrinos is not taken into account. The uncertainties shown by the vertical bars are from the number of events available in the sample, while the horizontal bars show the bin width. Some of the vertical bars are smaller than the markers and are not shown.

HPS reconstruction [43]. The online HLT version of DeepTau adopts the same approach, except that only the discriminant against jets is used. DeepTau combines information from the high-level features of the reconstructed τ_h candidate with the low-level information from the inner tracker, calorimeters, and muon subdetectors using PF candidates, electrons, and muons reconstructed within the τ_h candidate's isolation cone.

To ensure any analysis with final-state hadronic tau lepton decays could benefit from the DeepTau algorithm, the training is performed on a balanced mixture of electron, muon, τ_h candidates, and jets from MC datasets. Simulated samples of DY, $t\bar{t}$, and W+jet are used for genuine hadronic tau lepton decays. Simulated $t\bar{t}$ decays with one or two light leptons (e or μ) and QCD samples are used for electrons, muons, and jets misidentified as hadronic tau lepton decays, respectively.

In order to train the DeepTau algorithm such that it is suitable for a wide kinematic range, balance in the type of the τ_h candidates and their respective p_T and η is crucial. Available samples show diverse compositions of τ_h candidate decay modes and p_T–η distributions, with more events available in the low-p_T and central-η regions, and fewer events in the high-p_T and high-η regions. In order to ensure a uniform contribution from different samples, decay modes, and p_T–η bins, additional weights are used in the training.

7.1 Network architecture

The HLT DeepTau algorithm largely follows the offline version. The inputs are formatted in the η–ϕ plane in the same way as the offline DeepTau algorithm, with an "isolation cone" composed of an outer grid of 21×21 cells with $\Delta\eta\times\Delta\phi$ grid sizes of 0.05×0.05, and a "signal cone" with dense inner grid of 11×11 cells with $\Delta\eta\times\Delta\phi$ grid sizes of 0.02×0.02. To reduce the computing cost for the algorithm, the two grids are not allowed to overlap. Using a denser inner grid exploits the signal tau lepton decay products that are usually within a $\Delta R \approx 0.1$ cone on the η–ϕ plane. A dense inner grid also copes

2026 JINST 21 P04002

well with high-p_T jets whose constituents are collimated. The radius of the signal cone is defined as $R_{sig} = 3\,\text{GeV}/p_T$, with minimum and maximum allowed values of 0.05 and 0.1, while the isolation cone is defined as the remaining range from the edge of R_{sig} to $R = 0.5$. Three different subnetworks are constructed to be able to independently process the inputs from the high-level variables, the outer cells, and the inner cells. The outputs from the three subnetworks are concatenated and passed through four fully connected layers with 200 nodes each. The results are collected in a final layer with four nodes that yield the outputs. A softmax activation function [67] is then applied to yield estimates of the probabilities for the τ_h candidate to come from each of the four target classes: τ_h, jet, e, and μ.

For usage of DeepTau at the HLT, some simplifications in the inputs of the network were made. Because an individual HLT path must rely on the objects it produces, it is not possible to access reconstructed electrons and muons for every τ_h candidate at the HLT. Consequently, the electron and muon discriminants are not used in the online DeepTau algorithm. Leptons being misidentified as τ_h candidates are however not a leading background. Similarly, association and quality fits of the primary vertex for online PF candidates are not performed due to the online processing time constraint. Additionally, several track-related variables, such as d_z, are not used in the online DeepTau algorithm either. Despite these limitations, the DeepTau network still performs successfully, retaining high performance with the features available online.

7.2 Performance of the DeepTau algorithm

The performance of several τ_h HLT paths equipped with online DeepTau identification is presented in terms of event rate and HLT path efficiency. The working point is optimized for each HLT path to maximize the signal efficiency under the constraint that the HLT path retains an event rate similar to its Run 2 value. The optimization of the DeepTau identification thresholds is performed as a function of the τ_h candidate p_T.

Table 3. Rate estimation and observation for several τ_h HLT paths. Similarly to table 2, column A scales Run 2 data collected by the cut-based algorithm to Run 3 conditions, column B re-emulates Run 2 data using the L2TauNNTag algorithm and scales the result to Run 3 conditions, and column C is the evaluated rate in Run 3. The instantaneous luminosities used for the Run 2 estimation, Run 3 projection, and Run 3 evaluation were 1.68, 2.00, and $2.20 \times 10^{34}\,\text{cm}^{-2}\,\text{s}^{-1}$, respectively. The rates are inclusive calculations not excluding shared contributions from other algorithms or paths. The statistical uncertainties are negligible with respect to the significant digits reported.

HLT path	A [Hz]	B [Hz]	C [Hz]
$e\tau_h$	10	9	10
$\mu\tau_h$	5	5	5
Single-τ_h	14	13	15
Di-τ_h	55	46	51

Several τ_h HLT path rates are shown in table 3. The estimated DeepTau rates are computed using a dataset dedicated to rate estimates, collected in October 2018, corresponding to 2 hours of data taking at an average pileup of 47. This rate was then scaled to the expected Run 3 conditions, targeting a pileup of 60. The observed DeepTau rates are computed using a dataset collected in November 2022, corresponding to 4.5 hours of data taking at an average pileup of 54. A comparison of the overall efficiency between DeepTau and the Run 2 cut-based approach is shown in figure 5, where

2026 JINST 21 P04002

the L2TauNNTag filter is disabled in order to focus on the DeepTau performance. The efficiencies are evaluated using MC samples of $H \to \tau\tau$ and BSM $Z' \to \tau\tau$ events, simulated with early Run 3 conditions. In the presence of two τ_h candidates, the one with greater p_T is used in the calculation. The HLT paths using DeepTau are shown to outperform those using the Run 2 cut-based selection in the majority of the p_T range, while maintaining a similar event rate.

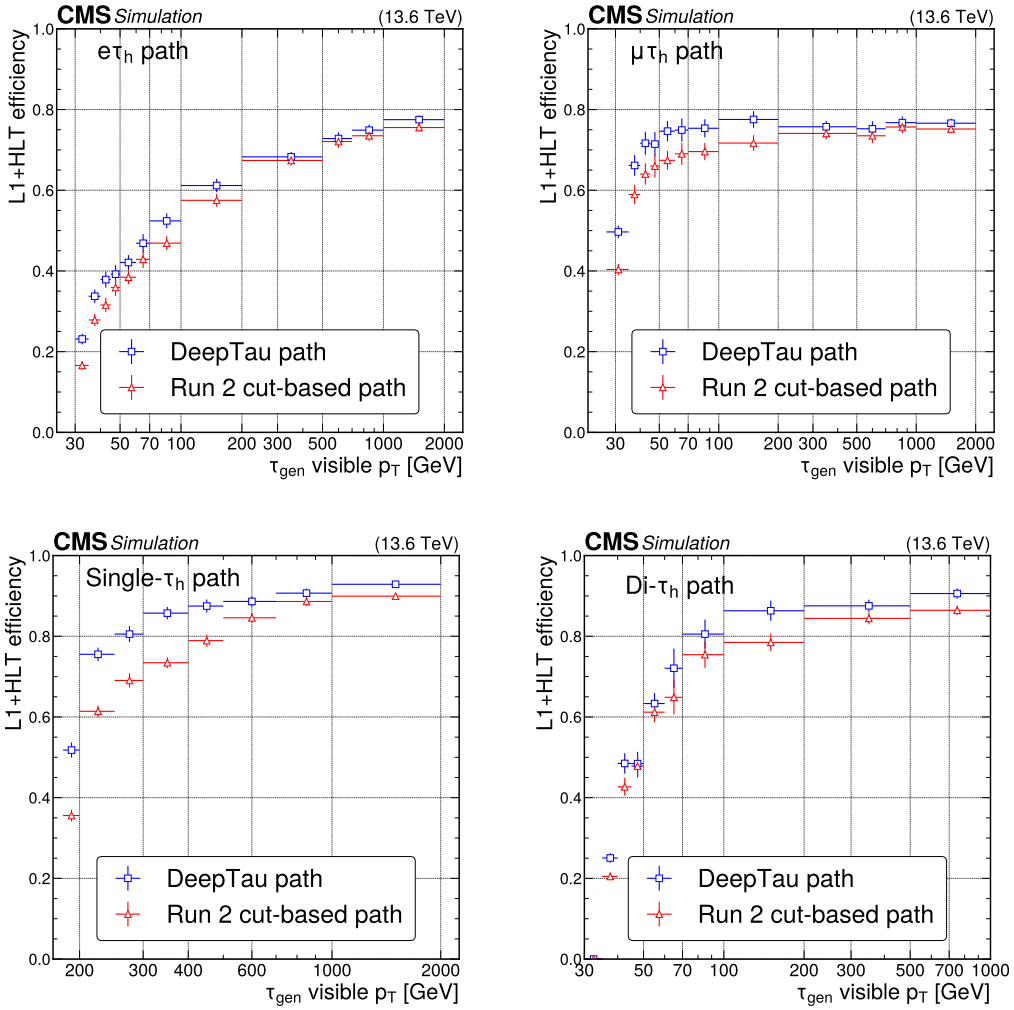

Figure 5. Total L1+HLT path efficiency of the $e\tau_h$ (upper left), $\mu\tau_h$ (upper right), single-τ_h (lower left), and di-τ_h (lower right) HLT paths as a function of the visible generator-level τ_h p_T, where "visible" refers to the fact that the contribution of neutrinos is not taken into account. The $H \to \tau\tau$ and BSM $Z' \to \tau\tau$ samples are used in the evaluation. The uncertainties shown by the vertical bars are from the number of events available in the sample, while the horizontal bars show the bin width. Some of the vertical bars are smaller than the markers and are not shown.

2026 JINST 21 P04002

8 Overall performance of the τ_h HLT paths

The performance studies presented in this section use pp collision data from 2022–2023. For all HLT paths, a "tag-and-probe" technique is used to measure the trigger efficiency [18, 68]. With this method, one first selects a tag object that satisfies stringent requirements, and then selects the probe object, whose efficiency is measured. In the case of τ_h HLT paths, the tag object used is always a muon, which is a well-isolated object highly distinguishable against jets. To perform this measurement in situ, so-called monitoring HLT paths are made which require one muon and one τ_h candidate. Each τ_h HLT path has a corresponding monitoring HLT path with the exact same τ_h candidate requirements. In this manner, the tag-and-probe method is applied to the monitoring HLT paths, and the measured efficiencies correspond to the signal HLT paths. This approach was validated using MC samples by comparing the signal HLT path efficiencies to the monitoring HLT path efficiencies collected with the tag-and-probe method, and the results were found to agree within uncertainties.

8.1 Efficiencies in experiment

The efficiency is measured from a region enriched in DY events, where the Z boson decays into two τ leptons that subsequently decay into a $\mu\tau_h$ final state. The tag muon is required to have $p_T > 24\,\text{GeV}$, $|\eta| < 2.4$, and be isolated such that nearby calorimeter energy deposits sum to less than 15% of the muon's p_T. Additionally, the tag muon is required to be within $\Delta R < 0.5$ of the muon reconstructed by the single muon HLT path, and pass the Medium ID for offline muons [23]. The probe τ_h candidate has the offline selection of $p_T > 20\,\text{GeV}$, $|\eta| < 2.1$, and passes the following offline DeepTau working points: VVLoose (Very Very Loose) against electrons, Tight against muons, and Medium against jets [43], summarized as "Offline Medium WP DeepTau ID applied" in relevant figures. Each working point corresponds to a specific trade-off between τ_h selection efficiency and background rejection rate. The muon and τ_h candidate must have opposite charges. A visible invariant mass window is required with $40 < m_{\text{vis}}(\mu, \tau_h) < 80\,\text{GeV}$ to reduce the efficiency impact of energy loss from neutrinos. To reduce the background contamination from W+jet processes, the event is also required to have a transverse mass less than 30 GeV, which is defined by the muon and $\vec{p}_T^{\,\text{miss}}$ as $m_T(\vec{p}_T^{\,\mu}, \vec{p}_T^{\,\text{miss}}) = \sqrt{2 p_T^{\mu} p_T^{\text{miss}} [1 - \cos\Delta\phi(\vec{p}_T^{\,\mu}, \vec{p}_T^{\,\text{miss}})]}$. The denominator of the efficiency includes all the $\mu\tau_h$ events passing the above selections, and the numerator includes the events also passing the relevant monitoring HLT path with the offline τ_h candidate matched to the τ_h candidate reconstructed at the HLT with $\Delta R < 0.5$. The efficiency of the single-τ_h HLT path cannot be measured with this method due to its high p_T threshold, resulting in few suitable events. It is measured with an alternative strategy selecting events with large p_T^{miss} that include $W \to \tau_h \nu_\tau$ decays.

The efficiencies of the τ_h leg in the $e\tau_h$ and $\mu\tau_h$ HLT paths are shown in figures 6 and 7, respectively, for 2022 and 2023. The absolute path efficiency is calculated, which includes the L1+HLT τ_h candidate efficiency. The $e\tau_h$ ($\mu\tau_h$) cross trigger has an online τ_h candidate p_T threshold of 30 (27) GeV; in addition to the offline selections for the τ_h candidate described above, the τ_h candidate is required to satisfy $p_T > 35$ (30) GeV for the efficiency measurements as a function of η, ϕ, and the number of primary vertices (N_{PV}). This reduces the impact of the low efficiency "turn-on" region of the HLT path, where events start to meet the threshold of passing the HLT path. The efficiency is robust against pileup, indicated by a stable N_{PV} plot, and the performance between the two years is comparable despite slightly different detector conditions.

2026 JINST 21 P04002

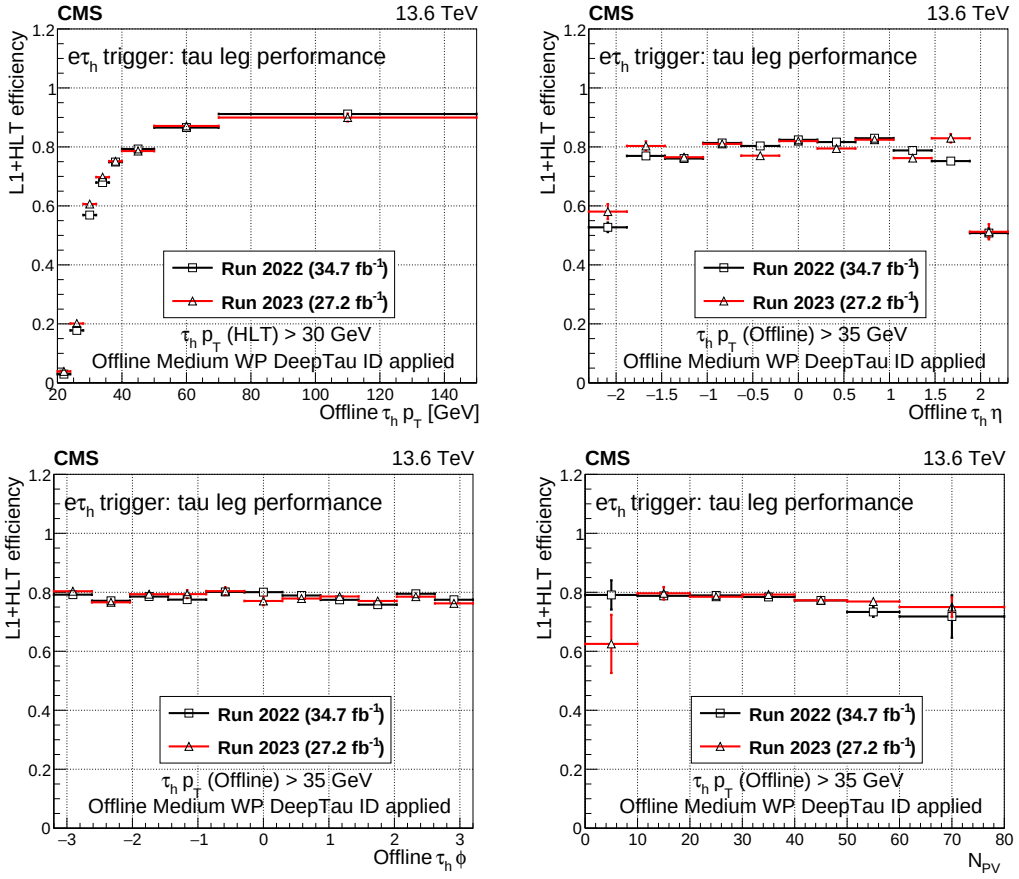

Figure 6. A comparison of the L1+HLT efficiency of the $e\tau_h$ monitoring HLT path in 2022 and 2023 as a function of offline τ_h candidate p_T (upper left), η (upper right), and ϕ (lower left). The dependence on the N_{PV} is also shown (lower right). The uncertainties shown by the vertical bars are from the number of events available in the sample, while the horizontal bars show the bin width. Some of the vertical bars are smaller than the markers and are not shown.

2026 JINST 21 P04002

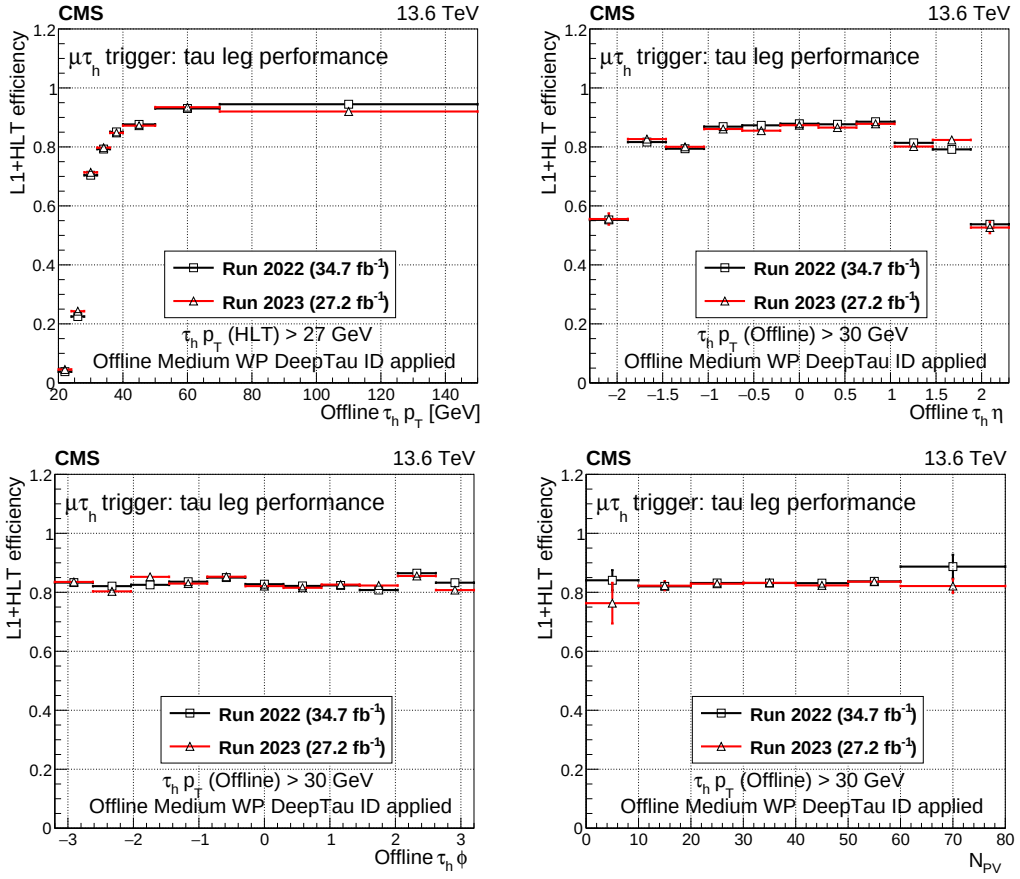

Figure 7. A comparison of the L1+HLT efficiency of the $\mu\tau_h$ HLT path in 2022 and 2023 as a function of offline τ_h candidate p_T (upper left), η (upper right), and ϕ (lower left). The dependence on the N_{PV} is also shown (lower right). The uncertainties shown by the vertical bars are from the number of events available in the sample, while the horizontal bars show the bin width. Some of the vertical bars are smaller than the markers and are not shown.

2026 JINST 21 P04002

The efficiency of the τ_h leg in the di-τ_h HLT path is shown in figure 8, for 2022 and 2023. A modified version of the di-τ_h HLT path was produced for Run 3, called di-τ_h+jet. It has online kinematic thresholds for τ_h candidates 5 GeV lower than the di-τ_h HLT path, and the additional requirement of an online jet with $p_T > 50$ GeV. This topology collects more low-p_T τ_h candidates than would be possible with the di-τ_h HLT path alone, at the cost of also requiring an energetic jet to reduce the HLT path's rate. The efficiency of the τ_h leg in this di-τ_h+jet HLT path is shown in figure 9, for 2022 and 2023. The HLT paths are evaluated in the same manner as the eτ_h and $\mu\tau_h$ HLT paths previously, with the only differences being the higher online p_T thresholds of 35 (30) GeV for the di-τ_h (di-τ_h+jet) HLT path, and offline τ_h candidate p_T threshold of 50 GeV. Again, the HLT path is found to plateau, be robust against pileup, and have consistent performance between the two years of collected data.

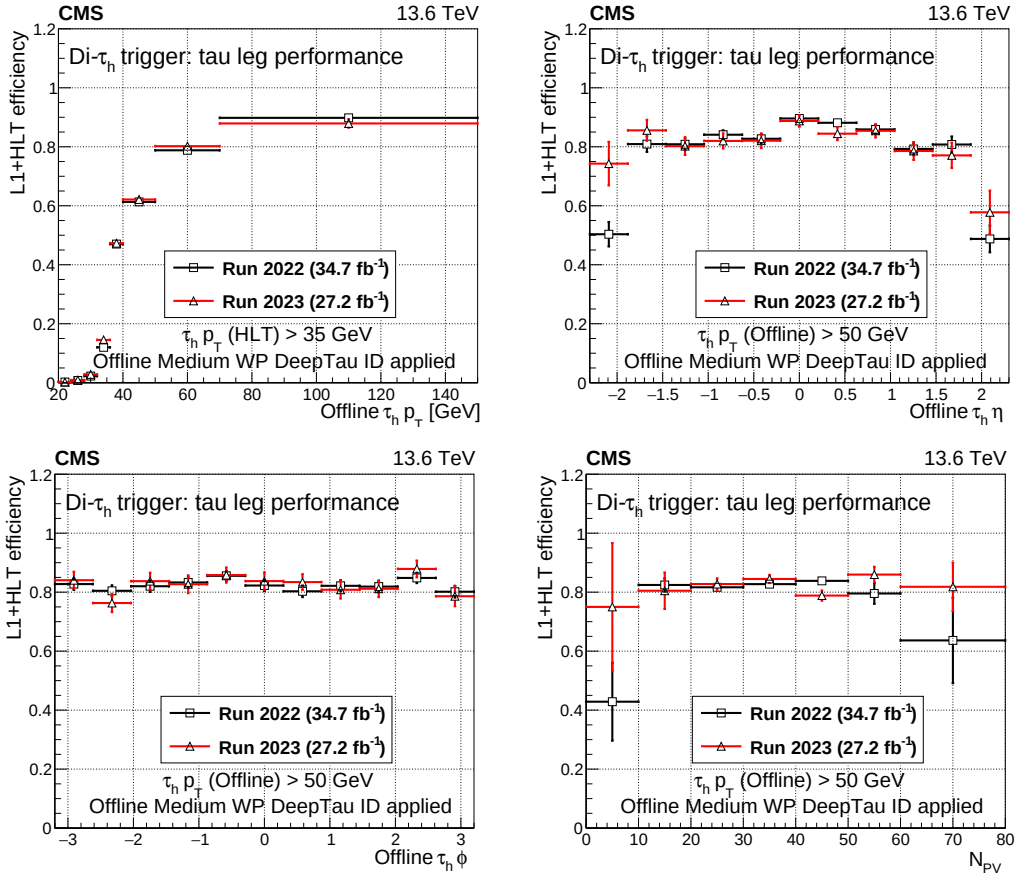

Figure 8. A comparison of the L1+HLT efficiency of the di-τ_h monitoring HLT path in 2022 and 2023 as a function of offline τ_h candidate p_T (upper left), η (upper right), and ϕ (lower left). The dependence on the N_{PV} is also shown (lower right). The uncertainties shown by the vertical bars are from the number of events available in the sample, while the horizontal bars show the bin width. Some of the vertical bars are smaller than the markers and are not shown.

2026 JINST 21 P04002

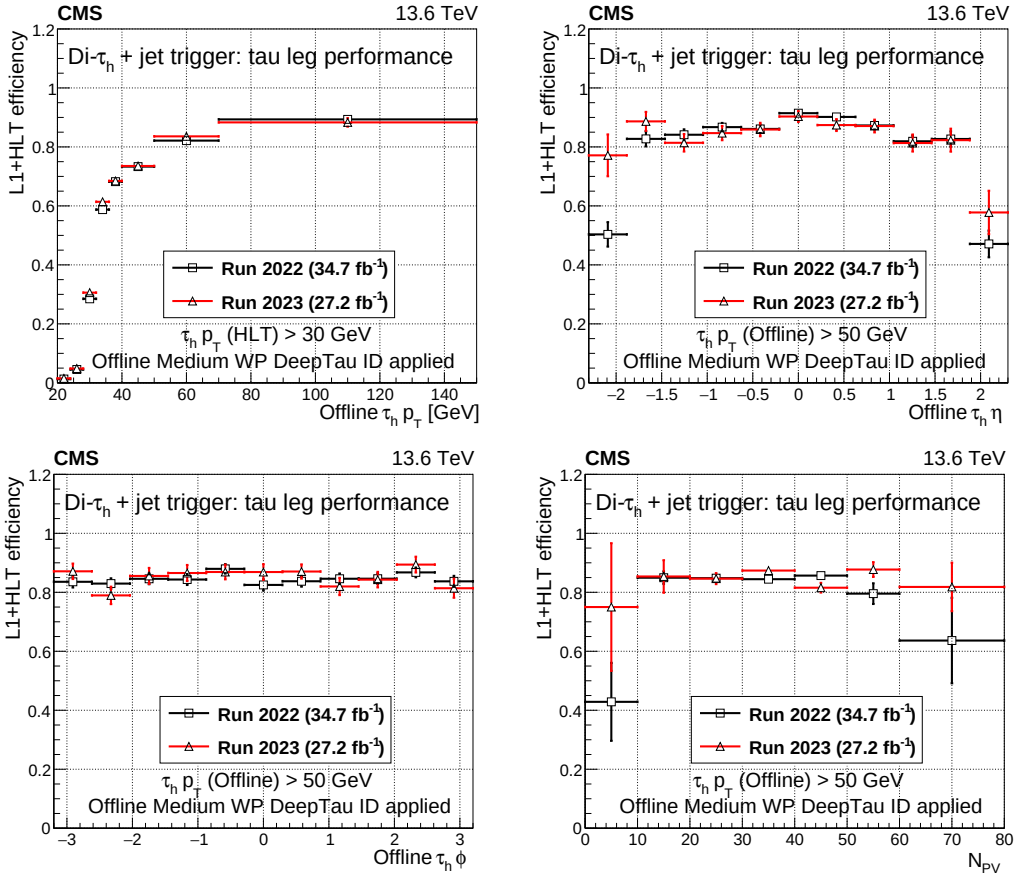

Figure 9. A comparison of the L1+HLT efficiency of the di-τ_h+jet monitoring HLT path in 2022 and 2023 as a function of offline τ_h candidate p_T (upper left), η (upper right), and ϕ (lower left). The dependence on the N_{PV} is also shown (lower right). The uncertainties shown by the vertical bars are from the number of events available in the sample, while the horizontal bars show the bin width. Some of the vertical bars are smaller than the markers and are not shown.

2026 JINST 21 P04002

8.2 Efficiencies in simulation

The efficiencies calculated with data from the previous subsection are now compared to efficiencies from simulation, using the same selection criteria as previously described per HLT path, and derived in the same DY enriched control region from the previous section. The purpose of the comparison is to identify and measure differences between data and simulation, directly illustrated in a ratio of the efficiencies. This ratio is called a scale factor, and is used together with its respective triggers to improve the accuracy of the detector response in simulation as compared with experiment. These scale factors are used in any analysis that uses the τ_h HLT paths.

The τ_h leg efficiencies and the corresponding scale factors of the $e\tau_h$, $\mu\tau_h$, di-τ_h, and di-τ_h+jet HLT paths are shown in figure 10 for the 2022–2023 data combined. Here, the fitting is performed using a Gaussian process regressor. To avoid unreliable extrapolations, step functions are introduced to smoothly concatenate the low- and high-p_T regions. The dominant source of uncertainty is from the statistical uncertainties in data and simulation. The scale factors are found to be close to unity after the turn-on, indicating a good description of τ_h HLT paths in simulation. The difference between data and simulation in the low-p_T region, below 60 GeV, is mainly due to the limited accuracy of HCAL energy response modeling, affecting the HCAL L1 trigger primitives in 2022–2023 simulations.

9 Summary

Two online machine-learning algorithms, L2TauNNTag, described here for the first time, and DeepTau, have been deployed into the high level trigger (HLT) to select hadronically decaying tau lepton (τ_h) candidates. Their performance has been evaluated using the data collected by the CMS experiment in proton-proton collisions at $\sqrt{s} = 13.6$ TeV in 2022–2023, corresponding to an integrated luminosity of 62 fb^{-1}. Comparisons to simulation were performed and show good agreement with the collected data, validating the current understanding of the HLT paths involving τ_h candidates. The updated HLT paths are found to deliver improved τ_h candidate identification efficiency without significantly increasing computational cost or event rate, allowing more genuine hadronic tau lepton decays to be collected at roughly the same resource cost as in 2018. These improvements benefit physics studies targeting final states with hadronically decaying tau leptons, including precision measurements of the Higgs boson, and searches beyond the standard model.

2026 JINST 21 P04002

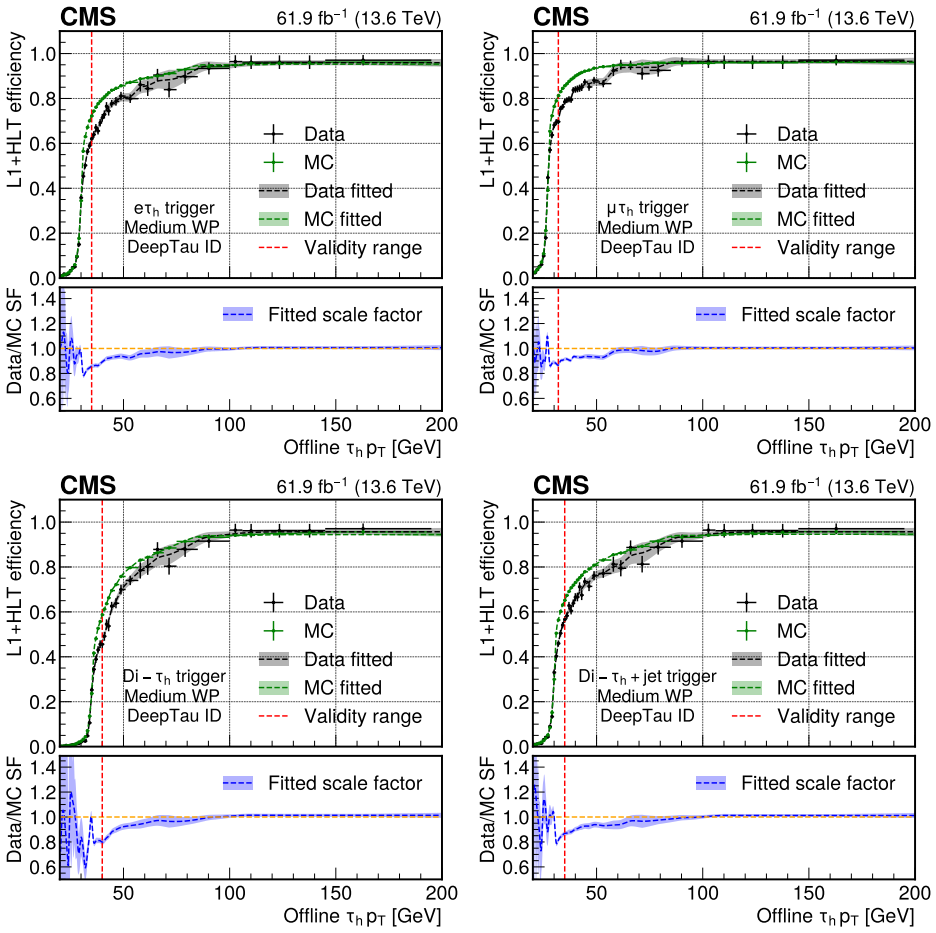

Figure 10. Efficiencies and scale factors of the HLT monitoring paths using 2022–2023 data as functions of the offline τ_h candidate p_T for the eτ_h (upper left), $\mu\tau_h$ (upper right), di-τ_h (lower left), and di-τ_h+jet (lower right) HLT paths. The measured efficiencies for data are shown with black markers, and for simulation with green markers. The uncertainties shown by the vertical bars are from the number of events available in the sample, while the horizontal bars show the bin width. Some of the vertical bars are smaller than the markers and are not shown. The systematic uncertainties are negligible with respect to the statistical uncertainties and are not included in the bands. The corresponding dotted lines of the same color display the best fit results together with the statistical uncertainty bands. The scale factors, defined as the ratios of efficiencies between data fitted and simulation fitted from the upper panels, are shown in the lower panels as blue lines with associated blue uncertainty bands. Only values to the right of the red dotted line are used in physics studies, to avoid large statistical fluctuations, as they are sufficiently above the turn-on threshold of the trigger.

2026 JINST 21 P04002

Acknowledgments

We congratulate our colleagues in the CERN accelerator departments for the excellent performance of the LHC and thank the technical and administrative staffs at CERN and at other CMS institutes for their contributions to the success of the CMS effort. In addition, we gratefully acknowledge the computing c,enters and personnel of the Worldwide LHC Computing Grid and other c,enters for delivering so effectively the computing infrastructure essential to our analyses. Finally, we acknowledge the enduring support for the construction and operation of the LHC, the CMS detector, and the supporting computing infrastructure provided by the following funding agencies: SC (Armenia), BMBWF and FWF (Austria); FNRS and FWO (Belgium); CNPq, CAPES, FAPERJ, FAPERGS, and FAPESP (Brazil); MES and BNSF (Bulgaria); CERN; CAS, MoST, and NSFC (China); MINCIENCIAS (Colombia); MSES and CSF (Croatia); RIF (Cyprus); SENESCYT (Ecuador); ERC PRG and PSG, TARISTU24-TK10 and MoER TK202 (Estonia); Academy of Finland, MEC, and HIP (Finland); CEA and CNRS/IN2P3 (France); SRNSF (Georgia); BMFTR, DFG, and HGF (Germany); GSRI (Greece); NKFIH (Hungary); DAE and DST (India); IPM (Iran); SFI (Ireland); INFN (Italy); MSIT and NRF (Republic of Korea); MES (Latvia); LMTLT (Lithuania); MOE and UM (Malaysia); BUAP, CINVESTAV, CONACYT, LNS, SEP, and UASLP-FAI (Mexico); MOS (Montenegro); MBIE (New Zealand); PAEC (Pakistan); MES, NSC, and NAWA (Poland); FCT (Portugal); MESTD (Serbia); MICIU/AEI and PCTI (Spain); MOSTR (Sri Lanka); Swiss Funding Agencies (Switzerland); MST (Taipei); MHESI (Thailand); TUBITAK and TENMAK (Türkiye); NASU (Ukraine); STFC (United Kingdom); DOE and NSF (U.S.A.).

Individuals have received support from the Marie-Curie program and the European Research Council and Horizon 2020 Grant, contract Nos. 675440, 724704, 752730, 758316, 765710, 824093, 101115353, 101002207, 101001205, and COST Action CA16108 (European Union); the Leventis Foundation; the Alfred P. Sloan Foundation; the Alexander von Humboldt Foundation; the Science Committee, project no. 22rl-037 (Armenia); the Fonds pour la Formation à la Recherche dans l'Industrie et dans l'Agriculture (FRIA) and Fonds voor Wetenschappelijk Onderzoek contract No. 1228724N (Belgium); the Beijing Municipal Science & Technology Commission, No. Z191100007219010, the Fundamental Research Funds for the Central Universities, the Ministry of Science and Technology of China under Grant No. 2023YFA1605804, the Natural Science Foundation of China under Grant No. 12535004, and USTC Research Funds of the Double First-Class Initiative No. YD2030002017 (China); the Ministry of Education, Youth and Sports (MEYS) of the Czech Republic; the Shota Rustaveli National Science Foundation, grant FR-22-985 (Georgia); the Deutsche Forschungsgemeinschaft (DFG), among others, under Germany's Excellence Strategy – EXC 2121 "Quantum Universe" – 390833306, and under project number 400140256 – GRK2497; the Hellenic Foundation for Research and Innovation (HFRI), Project Number 2288 (Greece); the Hungarian Academy of Sciences, the New National Excellence Program – ÚNKP, the NKFIH research grants K 131991, K 133046, K 138136, K 143460, K 143477, K 146913, K 146914, K 147048, 2020-2.2.1-ED-2021-00181, TKP2021-NKTA-64, and 2025-1.1.5-NEMZ_KI-2025-00004 (Hungary); the Council of Science and Industrial Research, India; ICSC – National Research C,enter for High Performance Computing, Big Data and Quantum Computing, FAIR – Future Artificial Intelligence Research, and CUP I53D23001070006 (Mission 4 Component 1), funded by the NextGenerationEU program (Italy); the Latvian Council of Science; the Ministry of Education and Science, project no. 2022/WK/14, and the National Science Center, contracts Opus 2021/41/B/ST2/01369, 2021/43/B/ST2/01552, 2023/49/B/ST2/03273, and the NAWA contract

2026 JINST 21 P04002

BPN/PPO/2021/1/00011 (Poland); the Fundação para a Ciência e a Tecnologia (Portugal); the National Priorities Research Program by Qatar National Research Fund; MICIU/AEI/10.13039/501100011033, ERDF/EU, "European Union NextGenerationEU/PRTR", and Programa Severo Ochoa del Principado de Asturias (Spain); the Chulalongkorn Academic into Its 2nd Century Project Advancement Project, the National Science, Research and Innovation Fund program IND_FF_68_369_2300_097, and the Program Management Unit for Human Resources & Institutional Development, Research and Innovation, grant B39G680009 (Thailand); the Eric & Wendy Schmidt Fund for Strategic Innovation through the CERN Next Generation Triggers project under grant agreement number SIF-2023-004; the Kavli Foundation; the Nvidia Corporation; the SuperMicro Corporation; the Welch Foundation, contract C-1845; and the Weston Havens Foundation (U.S.A.).

Data Availability Statement. Release and preservation of data used by the CMS Collaboration as the basis for publications is guided by the CMS data preservation, re-use and open access policy.

Code Availability Statement. The CMS core software is publicly available on GitHub.

References

[1] CMS collaboration, *Observation of the Higgs boson decay to a pair of τ leptons with the CMS detector*, *Phys. Lett. B* **779** (2018) 283 [arXiv:1708.00373].

[2] CMS collaboration, *Search for Higgs boson pair production in events with two bottom quarks and two tau leptons in proton-proton collisions at $\sqrt{s}$ = 13 TeV*, *Phys. Lett. B* **778** (2018) 101 [arXiv:1707.02909].

[3] ATLAS collaboration, *Cross-section measurements of the Higgs boson decaying into a pair of τ-leptons in proton-proton collisions at $\sqrt{s}$ = 13 TeV with the ATLAS detector*, *Phys. Rev. D* **99** (2019) 072001 [arXiv:1811.08856].

[4] ATLAS collaboration, *Search for resonant and non-resonant Higgs boson pair production in the $b\bar{b}\tau^+\tau^-$ decay channel in pp collisions at $\sqrt{s}$ = 13 TeV with the ATLAS detector*, *Phys. Rev. Lett.* **121** (2018) 191801 [*Erratum ibid.* **122** (2019) 089901] [arXiv:1808.00336].

[5] ATLAS collaboration, *Test of CP invariance in vector-boson fusion production of the Higgs boson in the $H \to \tau\tau$ channel in proton-proton collisions at $\sqrt{s}$ = 13 TeV with the ATLAS detector*, *Phys. Lett. B* **805** (2020) 135426 [arXiv:2002.05315].

[6] CMS collaboration, *Measurement of the production cross section of a Higgs boson with large transverse momentum in its decays to a pair of τ leptons in proton-proton collisions at $\sqrt{s}$ = 13 TeV*, *Phys. Lett. B* **857** (2024) 138964 [arXiv:2403.20201].

[7] CMS collaboration, *Search for Higgs boson pairs decaying to WW^*WW^*, $WW^*\tau\tau$, and $\tau\tau\tau\tau$ in proton-proton collisions at $\sqrt{s}$ = 13 TeV*, *JHEP* **07** (2023) 095 [arXiv:2206.10268].

[8] CMS collaboration, *Observation of $\gamma\gamma \to \tau\tau$ in proton-proton collisions and limits on the anomalous electromagnetic moments of the τ lepton*, *Rept. Prog. Phys.* **87** (2024) 107801 [arXiv:2406.03975].

[9] ATLAS collaboration, *Observation of the $\gamma\gamma \to \tau\tau$ process in Pb+Pb collisions and constraints on the τ-lepton anomalous magnetic moment with the ATLAS detector*, *Phys. Rev. Lett.* **131** (2023) 151802 [arXiv:2204.13478].

[10] CMS collaboration, *Measurement of the τ lepton polarization in Z boson decays in proton-proton collisions at $\sqrt{s}$ = 13 TeV*, *JHEP* **01** (2024) 101 [arXiv:2309.12408].

2026 JINST 21 P04002

[11] ATLAS collaboration, *Measurement of τ polarisation in $Z/\gamma^* \to \tau\tau$ decays in proton-proton collisions at $\sqrt{s} = 8$ TeV with the ATLAS detector*, *Eur. Phys. J. C* **78** (2018) 163 [arXiv:1709.03490].

[12] ATLAS collaboration, *Measurement of τ polarization in $W \to \tau\nu$ decays with the ATLAS detector in pp collisions at $\sqrt{s} = 7$ TeV*, *Eur. Phys. J. C* **72** (2012) 2062 [arXiv:1204.6720].

[13] CMS collaboration, *Searches for additional Higgs bosons and for vector leptoquarks in $\tau\tau$ final states in proton-proton collisions at $\sqrt{s} = 13$ TeV*, *JHEP* **07** (2023) 073 [arXiv:2208.02717].

[14] ATLAS collaboration, *Search for heavy Higgs bosons decaying into two tau leptons with the ATLAS detector using pp collisions at $\sqrt{s} = 13$ TeV*, *Phys. Rev. Lett.* **125** (2020) 051801 [arXiv:2002.12223].

[15] Particle Data Group collaboration, *Review of particle physics*, *Phys. Rev. D* **110** (2024) 030001.

[16] CMS collaboration, *The CMS experiment at the CERN LHC*, 2008 *JINST* **3** S08004 [arXiv:1003.4038].

[17] CMS collaboration, *Development of the CMS detector for the CERN LHC Run 3*, 2024 *JINST* **19** P05064 [arXiv:2309.05466].

[18] CMS collaboration, *Performance of reconstruction and identification of τ leptons decaying to hadrons and ν_τ in pp collisions at $\sqrt{s} = 13$ TeV*, 2018 *JINST* **13** P10005 [arXiv:1809.02816].

[19] CMS collaboration, *Performance of the CMS Level-1 trigger in proton-proton collisions at $\sqrt{s} = 13$ TeV*, 2020 *JINST* **15** P10017 [arXiv:2006.10165].

[20] CMS collaboration, *The CMS trigger system*, 2017 *JINST* **12** P01020 [arXiv:1609.02366].

[21] CMS collaboration, *Performance of the CMS high-level trigger during LHC Run 2*, 2024 *JINST* **19** P11021 [arXiv:2410.17038].

[22] CMS collaboration, *Electron and photon reconstruction and identification with the CMS experiment at the CERN LHC*, 2021 *JINST* **16** P05014 [arXiv:2012.06888].

[23] CMS collaboration, *Performance of the CMS muon detector and muon reconstruction with proton-proton collisions at $\sqrt{s} = 13$ TeV*, 2018 *JINST* **13** P06015 [arXiv:1804.04528].

[24] CMS collaboration, *Description and Performance of Track and Primary-Vertex Reconstruction with the CMS Tracker*, 2014 *JINST* **9** P10009 [arXiv:1405.6569].

[25] CMS collaboration, *CMS Technical Design Report for the Phase 1 Upgrade of the Hadron Calorimeter*, CERN-LHCC-2012-015 (2012) [DOI:10.2172/1151651].

[26] CMS collaboration, *Performance of the CMS Phase-1 pixel detector with Run 3 data*, CMS Detector Performance Note CMS-DP-2022-047 (2022).

[27] CMS collaboration, *Commissioning CMS online reconstruction with GPUs*, CMS Detector Performance Note CMS-DP-2023-004 (2022).

[28] CMS BRIL collaboration, *The Pixel Luminosity Telescope: a detector for luminosity measurement at CMS using silicon pixel sensors*, *Eur. Phys. J. C* **83** (2023) 673 [arXiv:2206.08870].

[29] CMS collaboration, *Run 3 luminosity measurements with the Pixel Luminosity Telescope*, *PoS* **ICHEP2022** (2022) 936.

[30] CMS collaboration, *Upgraded CMS Fast Beam Condition Monitor for LHC Run 3 Online Luminosity and Beam Induced Background Measurements*, *JACoW I* **BIC2022** (2022) 540.

[31] CMS collaboration, *Particle-flow reconstruction and global event description with the CMS detector*, 2017 *JINST* **12** P10003 [arXiv:1706.04965].

[32] D. Contardo et al., *Technical Proposal for the Phase-II Upgrade of the CMS Detector*, CERN-LHCC-2015-010 (2015) [DOI:10.17181/CERN.VU8I.D59J].

2026 JINST 21 P04002

[33] M. Cacciari, G.P. Salam and G. Soyez, *The anti-k_t jet clustering algorithm*, *JHEP* **04** (2008) 063 [arXiv:0802.1189].

[34] M. Cacciari, G.P. Salam and G. Soyez, *FastJet User Manual*, *Eur. Phys. J. C* **72** (2012) 1896 [arXiv:1111.6097].

[35] CMS collaboration, *Pileup mitigation at CMS in 13 TeV data*, 2020 *JINST* **15** P09018 [arXiv:2003.00503].

[36] D. Bertolini, P. Harris, M. Low and N. Tran, *Pileup Per Particle Identification*, *JHEP* **10** (2014) 059 [arXiv:1407.6013].

[37] CMS collaboration, *Jet energy scale and resolution in the CMS experiment in pp collisions at 8 TeV*, 2017 *JINST* **12** P02014 [arXiv:1607.03663].

[38] CMS collaboration, *Performance of electron reconstruction and selection with the CMS detector in proton-proton collisions at* $\sqrt{s} = 8$ *TeV*, 2015 *JINST* **10** P06005 [arXiv:1502.02701].

[39] CMS collaboration, *Performance of missing transverse momentum reconstruction in proton-proton collisions at* $\sqrt{s} = 13$ *TeV using the CMS detector*, 2019 *JINST* **14** P07004 [arXiv:1903.06078].

[40] CMS collaboration, *Performance of τ-lepton reconstruction and identification in CMS*, 2012 *JINST* **7** P01001 [arXiv:1109.6034].

[41] CMS collaboration, *Reconstruction and identification of τ lepton decays to hadrons and ν_τ at CMS*, 2016 *JINST* **11** P01019 [arXiv:1510.07488].

[42] CMS collaboration, *Performance of the DeepTau algorithm for the discrimination of taus against jets, electron, and muons*, CMS Detector Performance Note CMS-DP-2019-033 (2019).

[43] CMS collaboration, *Identification of hadronic tau lepton decays using a deep neural network*, 2022 *JINST* **17** P07023 [arXiv:2201.08458].

[44] CMS collaboration, *Luminosity measurement in proton-proton collisions at* 13.6 *TeV in 2022 at CMS*, CMS-PAS-LUM-22-001 (2024).

[45] CMS collaboration, *Measurement of the offline integrated luminosity for the CMS proton-proton collision dataset recorded in 2023*, CMS Detector Performance Note CMS-DP-2024-068 (2024).

[46] CMS collaboration, *Luminosity determination using Z boson production at the CMS experiment*, *Eur. Phys. J. C* **84** (2024) 26 [arXiv:2309.01008].

[47] CMS collaboration, *Precision luminosity measurement in proton-proton collisions at* $\sqrt{s} = 13$ *TeV in 2015 and 2016 at CMS*, *Eur. Phys. J. C* **81** (2021) 800 [arXiv:2104.01927].

[48] J. Alwall et al., *The automated computation of tree-level and next-to-leading order differential cross sections, and their matching to parton shower simulations*, *JHEP* **07** (2014) 079 [arXiv:1405.0301].

[49] J. Alwall et al., *Comparative study of various algorithms for the merging of parton showers and matrix elements in hadronic collisions*, *Eur. Phys. J. C* **53** (2008) 473 [arXiv:0706.2569].

[50] T. Sjöstrand et al., *An introduction to PYTHIA 8.2*, *Comput. Phys. Commun.* **191** (2015) 159 [arXiv:1410.3012].

[51] P. Nason, *A new method for combining NLO QCD with shower Monte Carlo algorithms*, *JHEP* **11** (2004) 040 [hep-ph/0409146].

[52] S. Frixione, P. Nason and C. Oleari, *Matching NLO QCD computations with Parton Shower simulations: the POWHEG method*, *JHEP* **11** (2007) 070 [arXiv:0709.2092].

[53] S. Alioli, P. Nason, C. Oleari and E. Re, *A general framework for implementing NLO calculations in shower Monte Carlo programs: the POWHEG BOX*, *JHEP* **06** (2010) 043 [arXiv:1002.2581].

2026 JINST 21 P04002

[54] J.M. Campbell, R.K. Ellis, P. Nason and E. Re, *Top-Pair Production and Decay at NLO Matched with Parton Showers*, *JHEP* **04** (2015) 114 [arXiv:1412.1828].

[55] S. Frixione, P. Nason and G. Ridolfi, *A Positive-weight next-to-leading-order Monte Carlo for heavy flavour hadroproduction*, *JHEP* **09** (2007) 126 [arXiv:0707.3088].

[56] P. Nason and C. Oleari, *NLO Higgs boson production via vector-boson fusion matched with shower in POWHEG*, *JHEP* **02** (2010) 037 [arXiv:0911.5299].

[57] CMS collaboration, *Extraction and validation of a new set of CMS PYTHIA8 tunes from underlying-event measurements*, *Eur. Phys. J. C* **80** (2020) 4 [arXiv:1903.12179].

[58] N. Davidson et al., *Universal Interface of TAUOLA Technical and Physics Documentation*, *Comput. Phys. Commun.* **183** (2012) 821 [arXiv:1002.0543].

[59] NNPDF collaboration, *Parton distributions for the LHC Run II*, *JHEP* **04** (2015) 040 [arXiv:1410.8849].

[60] NNPDF collaboration, *Parton distributions from high-precision collider data*, *Eur. Phys. J. C* **77** (2017) 663 [arXiv:1706.00428].

[61] GEANT4 collaboration, *GEANT4 — A Simulation Toolkit*, *Nucl. Instrum. Meth. A* **506** (2003) 250.

[62] CMS collaboration, *Performance of Level-1 trigger e/γ and τ in Run 3*, CMS Detector Performance Note CMS-DP-2023-008 (2023).

[63] A. Bocci et al., *Heterogeneous Reconstruction of Tracks and Primary Vertices With the CMS Pixel Tracker*, *Front. Big Data* **3** (2020) 601728 [arXiv:2008.13461].

[64] CMS Collaboration, *Performance of Run-3 HLT track reconstruction*, CMS Detector Performance Note CMS-DP-2022-014 (2022).

[65] D.P. Kingma and J. Ba, *Adam: A method for stochastic optimization*, in *3rd International Conference on Learning Representations, ICLR*, (2014) [arXiv:1412.6980].

[66] CMS collaboration, *Identification of tau leptons using a convolutional neural network with domain adaptation*, 2025 *JINST* **20** P12032 [arXiv:2511.05468].

[67] I.J. Goodfellow, Y. Bengio and A. Courville, *Deep Learning*, MIT Press, Cambridge, MA, U.S.A. (2016).

[68] CMS collaboration, *CMS RPC efficiency measurement using the tag-and-probe method*, 2019 *JINST* **14** C10020.

2026 JINST 21 P04002

The CMS collaboration

A. Hayrapetyan[1], V. Makarenko[1], A. Tumasyan[1,a], W. Adam[2], L. Benato[2], T. Bergauer[2], M. Dragicevic[2], P.S. Hussain[2], M. Jeitler[2,b], N. Krammer[2], A. Li[2], D. Liko[2], M. Matthewman[2], J. Schieck[2,b], R. Schöfbeck[2,b], M. Shooshtari[2], M. Sonawane[2], W. Waltenberger[2], C.-E. Wulz[2,b], T. Janssen[3], H. Kwon[3], D. Ocampo Henao[3], T. Van Laer[3], P. Van Mechelen[3], J. Bierkens[4], N. Breugelmans[4], J. D'Hondt[4], S. Dansana[4], A. De Moor[4], M. Delcourt[4], F. Heyen[4], Y. Hong[4], P. Kashko[4], S. Lowette[4], I. Makarenko[4], S. Tavernier[4], M. Tytgat[4,c], G.P. Van Onsem[4], S. Van Putte[4], D. Vannerom[4], B. Bilin[5], B. Clerbaux[5], A.K. Das[5], I. De Bruyn[5], G. De Lentdecker[5], H. Evard[5], L. Favart[5], P. Gianneios[5], A. Khalilzadeh[5], F.A. Khan[5], A. Malara[5], M.A. Shahzad[5], A. Sharma[5], L. Thomas[5], M. Vanden Bemden[5], C. Vander Velde[5], P. Vanlaer[5], F. Zhang[5], M. De Coen[6], D. Dobur[6], C. Giordano[6], G. Gokbulut[6], K. Kaspar[6], D. Kavtaradze[6], D. Marckx[6], K. Skovpen[6], A.M. Tomaru[6], N. Van Den Bossche[6], J. van der Linden[6], J. Vandenbroeck[6], H. Aarup Petersen[7], S. Bein[7], A. Benecke[7], A. Bethani[7], G. Bruno[7], A. Cappati[7], J. De Favereau De Jeneret[7], C. Delaere[7], F. Gameiro Casalinho[7], A. Giammanco[7], A.O. Guzel[7], V. Lemaitre[7], J. Lidrych[7], P. Malek[7], P. Mastrapasqua[7], S. Turkcapar[7], G.A. Alves[8], M. Barroso Ferreira Filho[8], E. Coelho[8], C. Hensel[8], D. Matos Figueiredo[8], T. Menezes De Oliveira[8], C. Mora Herrera[8], P. Rebello Teles[8], M. Soeiro[8], E.J. Tonelli Manganote[8,d], A. Vilela Pereira[8], W.L. Aldá Júnior[9], H. Brandao Malbouisson[9], W. Carvalho[9], J. Chinellato[9,e], M. Costa Reis[9], E.M. Da Costa[9], G.G. Da Silveira[9,f], D. De Jesus Damiao[9], S. Fonseca De Souza[9], R. Gomes De Souza[9], S. S. Jesus[9], T. Laux Kuhn[9,f], M. Macedo[9], K. Mota Amarilo[9], L. Mundim[9], H. Nogima[9], J.P. Pinheiro[9], A. Santoro[9], A. Sznajder[9], M. Thiel[9], F. Torres Da Silva De Araujo[9,g], C.A. Bernardes[10], L. Calligaris[10], F. Damas[10], E.M. Gregores[10], B. Lopes Da Costa[10], I. Maietto Silverio[10], P.G. Mercadante[10], S.F. Novaes[10], Sandra S. Padula[10], V. Scheurer[10], T.R. Fernandez Perez Tomei[10], A. Aleksandrov[11], G. Antchev[11], P. Danev[11], R. Hadjiiska[11], P. Iaydjiev[11], M. Shopova[11], G. Sultanov[11], A. Dimitrov[12], L. Litov[12], B. Pavlov[12], P. Petkov[12], A. Petrov[12], S. Keshri[13], D. Laroze[13], S. Thakur[13], W. Brooks[14], T. Cheng[15], T. Javaid[15], L. Wang[15], L. Yuan[15], Z. Hu[16], Z. Liang[16], J. Liu[16], X. Wang[16], H. Yang[16], G.M. Chen[17,h], H.S. Chen[17,h], M. Chen[17,h], Y. Chen[17], Q. Hou[17], X. Hou[17], F. Iemmi[17], C.H. Jiang[17], H. Liao[17], G. Liu[17], Z.-A. Liu[17,i], J.N. Song[17,i], S. Song[17], J. Tao[17], C. Wang[17,h], J. Wang[17], H. Zhang[17], J. Zhao[17], A. Agapitos[18], Y. Ban[18], A. Carvalho Antunes De Oliveira[18], S. Deng[18], B. Guo[18], Q. Guo[18], C. Jiang[18], A. Levin[18], C. Li[18], Q. Li[18], Y. Mao[18], S. Qian[18], S.J. Qian[18], X. Qin[18], C. Quaranta[18], X. Sun[18], D. Wang[18], J. Wang[18], M. Zhang[18], Y. Zhao[18], C. Zhou[18], S. Yang[19], Z. You[20], N. Lu[21], G. Bauer[22,j,k], Z. Cui[22,k], B. Li[22,l], H. Wang[22], K. Yi[22,m], J. Zhang[22], Y. Li[23], Y. Zhou[23,n], Z. Lin[24], C. Lu[24], M. Xiao[24,o], C. Avila[25], D.A. Barbosa Trujillo[25], A. Cabrera[25], C. Florez[25], J. Fraga[25], J.A. Reyes Vega[25], C. Rendón[26], M. Rodriguez[26], A.A. Ruales Barbosa[26], J.D. Ruiz Alvarez[26], N. Godinovic[27], D. Lelas[27], A. Sculac[27], M. Kovac[28], A. Petkovic[28], T. Sculac[28], P. Bargassa[29], V. Brigljevic[29], B.K. Chitroda[29], D. Ferencek[29], K. Jakovcic[29], A. Starodumov[29], T. Susa[29], A. Attikis[30], K. Christoforou[30], S. Konstantinou[30], C. Leonidou[30], L. Paizanos[30], F. Ptochos[30], P.A. Razis[30], H. Rykaczewski[30], H. Saka[30], A. Stepennov[30], M. Finger[31,†], M. Finger Jr.[31], E. Carrera Jarrin[32], A.A. Abdelalim[33,p,q], B. El-mahdy[33,r], A. Hussein[34], H. Mohammed[34], K. Jaffel[35], M. Kadastik[35], T. Lange[35], C. Nielsen[35], J. Pata[35], M. Raidal[35], N. Seeba[35], L. Tani[35], E. Brücken[36], A. Milieva[36], K. Osterberg[36], M. Voutilainen[36], F. Garcia[37], P. Inkaew[37], K.T.S. Kallonen[37],

2026 JINST 21 P04002

R. Kumar Verma[37], T. Lampén[37], K. Lassila-Perini[37], B. Lehtela[37], S. Lehti[37], T. Lindén[37], N.R. Mancilla Xinto[37], M. Myllymäki[37], M.m. Rantanen[37], S. Saariokari[37], N.T. Toikka[37], J. Tuominiemi[37], N. Bin Norjoharuddeen[38], H. Kirschenmann[38], P. Luukka[38], H. Petrow[38], M. Besancon[39], F. Couderc[39], M. Dejardin[39], D. Denegri[39], P. Devouge[39], J.L. Faure[39], F. Ferri[39], P. Gaigne[39], S. Ganjour[39], P. Gras[39], F. Guilloux[39], G. Hamel de Monchenault[39], M. Kumar[39], V. Lohezic[39], Y. Maidannyk[39], J. Malcles[39], F. Orlandi[39], L. Portales[39], S. Ronchi[39], M.Ö. Sahin[39], P. Simkina[39], M. Titov[39], M. Tornago[39], R. Amella Ranz[40], F. Beaudette[40], G. Boldrini[40], P. Busson[40], C. Charlot[40], M. Chiusi[40], T.D. Cuisset[40], O. Davignon[40], A. De Wit[40], T. Debnath[40], I.T. Ehle[40], S. Ghosh[40], A. Gilbert[40], R. Granier de Cassagnac[40], L. Kalipoliti[40], M. Manoni[40], M. Nguyen[40], S. Obraztsov[40], C. Ochando[40], R. Salerno[40], J.B. Sauvan[40], Y. Sirois[40], G. Sokmen[40], Y. Song[40], L. Urda Gómez[40], A. Zabi[40], A. Zghiche[40], J.-L. Agram[41,s], J. Andrea[41], D. Bloch[41], J.-M. Brom[41], E.C. Chabert[41], C. Collard[41], G. Coulon[41], S. Falke[41], U. Goerlach[41], R. Haeberle[41], A.-C. Le Bihan[41], M. Meena[41], O. Poncet[41], G. Saha[41], A. Savoy-Navarro[41,t], P. Vaucelle[41], A. Di Florio[42], B. Orzari[42], D. Amram[43], S. Beauceron[43], B. Blancon[43], G. Boudoul[43], N. Chanon[43], D. Contardo[43], P. Depasse[43], H. El Mamouni[43], J. Fay[43], E. Fillaudeau[43], S. Gascon[43], M. Gouzevitch[43], C. Greenberg[43], G. Grenier[43], B. Ille[43], E. Jourd'Huy[43], M. Lethuillier[43], B. Massoteau[43], L. Mirabito[43], A. Purohit[43], M. Vander Donckt[43], C. Verollet[43], J. Xiao[43], G. Adamov[44], I. Lomidze[44], Z. Tsamalaidze[44,u], V. Botta[45], S. Consuegra Rodríguez[45], L. Feld[45], K. Klein[45], M. Lipinski[45], P. Nattland[45], V. Oppenländer[45], A. Pauls[45], D. Pérez Adán[45], N. Röwert[45], C. Daumann[46], S. Diekmann[46], N. Eich[46], D. Eliseev[46], F. Engelke[46], J. Erdmann[46], M. Erdmann[46], B. Fischer[46], T. Hebbeker[46], K. Hoepfner[46], A. Jung[46], N. Kumar[46], M.y. Lee[46], F. Mausolf[46], M. Merschmeyer[46], A. Meyer[46], A. Pozdnyakov[46], W. Redjeb[46], H. Reithler[46], U. Sarkar[46], V. Sarkisovi[46], A. Schmidt[46], C. Seth[46], A. Sharma[46], J.L. Spah[46], V. Vaulin[46], S. Zaleski[46], M.R. Beckers[47], C. Dziwok[47], G. Flügge[47], N. Hoeflich[47], T. Kress[47], A. Nowack[47], O. Pooth[47], A. Stahl[47], A. Zotz[47], A. Abel[48], M. Aldaya Martin[48], J. Alimena[48], Y. An[48], I. Andreev[48], J. Bach[48], S. Baxter[48], H. Becerril Gonzalez[48], O. Behnke[48], A. Belvedere[48], F. Blekman[48,v], K. Borras[48,w], A. Campbell[48], S. Chatterjee[48], L.X. Coll Saravia[48], G. Eckerlin[48], D. Eckstein[48], E. Gallo[48,v], A. Geiser[48], M. Guthoff[48], A. Hinzmann[48], L. Jeppe[48], M. Kasemann[48], C. Kleinwort[48], R. Kogler[48], M. Komm[48], D. Krücker[48], W. Lange[48], D. Leyva Pernia[48], K.-Y. Lin[48], K. Lipka[48,x], W. Lohmann[48,y], J. Malvaso[48], R. Mankel[48], I.-A. Melzer-Pellmann[48], M. Mendizabal Morentin[48], A.B. Meyer[48], G. Milella[48], K. Moral Figueroa[48], A. Mussgiller[48], L.P. Nair[48], J. Niedziela[48], A. Nürnberg[48], J. Park[48], E. Ranken[48], A. Raspereza[48], D. Rastorguev[48], L. Rygaard[48], M. Scham[48,z,aa], S. Schnake[48,w], C. Schwanenberger[48,v], D. Schwarz[48], P. Schütze[48], D. Selivanova[48], K. Sharko[48], M. Shchedrolosiev[48], D. Stafford[48], M. Torkian[48], A. Ventura Barroso[48], R. Walsh[48], D. Wang[48], Q. Wang[48], K. Wichmann[48], L. Wiens[48,w], C. Wissing[48], Y. Yang[48], S. Zakharov[48], A. Zimermmane Castro Santos[48], A.R. Alves Andrade[49], M. Antonello[49], S. Bollweg[49], M. Bonanomi[49], L. Ebeling[49], K. El Morabit[49], Y. Fischer[49], M. Frahm[49], E. Garutti[49], A. Grohsjean[49], A.A. Guvenli[49], J. Haller[49], D. Hundhausen[49], G. Kasieczka[49], P. Keicher[49], R. Klanner[49], W. Korcari[49], T. Kramer[49], C.c. Kuo[49], F. Labe[49], J. Lange[49], A. Lobanov[49], J. Matthiesen[49], L. Moureaux[49], K. Nikolopoulos[49], A. Paasch[49], K.J. Pena Rodriguez[49], N. Prouvost[49], B. Raciti[49], M. Rieger[49], D. Savoiu[49], P. Schleper[49], M. Schröder[49],

2026 JINST 21 P04002

J. Schwandt[49], M. Sommerhalder[49], H. Stadie[49], G. Steinbrück[49], R. Ward[49], B. Wiederspan[49], M. Wolf[49], C. Yede[49], A. Brusamolino[50], E. Butz[50], Y.M. Chen[50], T. Chwalek[50], A. Dierlamm[50], G.G. Dincer[50], D. Druzhkin[50], U. Elicabuk[50], N. Faltermann[50], M. Giffels[50], A. Gottmann[50], F. Hartmann[50,ab], M. Horzela[50], F. Hummer[50], U. Husemann[50], J. Kieseler[50], M. Klute[50], J. Knolle[50], R. Kunnilan Muhammed Rafeek[50], O. Lavoryk[50], J.M. Lawhorn[50], S. Maier[50], M. Molch[50], A.A. Monsch[50], M. Mormile[50], Th. Müller[50], E. Pfeffer[50], M. Presilla[50], G. Quast[50], K. Rabbertz[50], B. Regnery[50], R. Schmieder[50], N. Shadskiy[50], I. Shvetsov[50], H.J. Simonis[50], L. Sowa[50], L. Stockmeier[50], K. Tauqeer[50], M. Toms[50], B. Topko[50], N. Trevisani[50], C. Verstege[50], T. Voigtländer[50], R.F. Von Cube[50], J. Von Den Driesch[50], C. Winter[50], R. Wolf[50], W.D. Zeuner[50], X. Zuo[50], G. Anagnostou[51], G. Daskalakis[51], A. Kyriakis[51], G. Melachroinos[52], Z. Painesis[52], I. Paraskevas[52], N. Saoulidou[52], K. Theofilatos[52], E. Tziaferi[52], E. Tzovara[52], K. Vellidis[52], I. Zisopoulos[52], T. Chatzistavrou[53], G. Karapostoli[53], K. Kousouris[53], E. Siamarkou[53], G. Tsipolitis[53], I. Bestintzanos[54], I. Evangelou[54], C. Foudas[54], P. Katsoulis[54], P. Kokkas[54], P.G. Kosmoglou Kioseoglou[54], N. Manthos[54], I. Papadopoulos[54], J. Strologas[54], C. Hajdu[55], D. Horvath[55,ac,ad], Á. Kadlecsik[55], C. Lee[55], K. Márton[55], A.J. Rádl[55,ae], F. Sikler[55], V. Veszpremi[55], M. Csanád[56], K. Farkas[56], A. Fehérkuti[56,af], M.M.A. Gadallah[56,ag], M. León Coello[56], G. Pásztor[56], G.I. Veres[56], B. Ujvari[57], G. Zilizi[57], G. Bencze[58], S. Czellar[58], J. Molnar[58], Z. Szillasi[58], T. Csorgo[59,af], F. Nemes[59,af], T. Novak[59], I. Szanyi[59,ah], S. Bahinipati[60], S. Nayak[60], R. Raturi[60], S. Bansal[61], S.B. Beri[61], V. Bhatnagar[61], S. Chauhan[61], N. Dhingra[61,ai], A. Kaur[61], H. Kaur[61], M. Kaur[61], S. Kumar[61], T. Sheokand[61], J.B. Singh[61], A. Singla[61], A. Bhardwaj[62], A. Chhetri[62], B.C. Choudhary[62], A. Kumar[62], A. Kumar[62], M. Naimuddin[62], S. Phor[62], K. Ranjan[62], M.K. Saini[62], P. Palni[63], S. Acharya[64,aj], B. Gomber[64], S. Mukherjee[65], S. Bhattacharya[66], S. Das Gupta[66], S. Dutta[66], S. Dutta[66], S. Sarkar[66], M.M. Ameen[67], P.K. Behera[67], S. Chatterjee[67], G. Dash[67], A. Dattamunsi[67], P. Jana[67], P. Kalbhor[67], S. Kamble[67], J.R. Komaragiri[67,ak], T. Mishra[67], P.R. Pujahari[67], A.K. Sikdar[67], R.K. Singh[67], P. Verma[67], S. Verma[67], A. Vijay[67], B.K. Sirasva[68], L. Bhatt[69], S. Dugad[69], G.B. Mohanty[69], M. Shelake[69], P. Suryadevara[69], A. Bala[70], S. Banerjee[70], S. Barman[70,al], R.M. Chatterjee[70], M. Guchait[70], Sh. Jain[70], A. Jaiswal[70], S. Kumar[70], M. Maity[70,al], G. Majumder[70], K. Mazumdar[70], S. Parolia[70], R. Saxena[70], A. Thachayath[70], D. Maity[71,am], P. Mal[71], K. Naskar[71,am], A. Nayak[71,am], K. Pal[71], P. Sadangi[71], S.K. Swain[71], S. Varghese[71,am], D. Vats[71,am], S. Dube[72], P. Hazarika[72], B. Kansal[72], A. Laha[72], R. Sharma[72], S. Sharma[72], K.Y. Vaish[72], S. Ghosh[73], H. Bakhshiansohi[74,an], A. Jafari[74,ao], V. Sedighzadeh Dalavi[74], M. Zeinali[74,ap], S. Bashiri[75], S. Chenarani[75,aq], S.M. Etesami[75], Y. Hosseini[75], M. Khakzad[75], E. Khazaie[75], M. Mohammadi Najafabadi[75], S. Tizchang[75,ar], M. Felcini[76], M. Grunewald[76], M. Abbrescia[77a,77b], M. Barbieri[77a,77b], M. Buonsante[77a,77b], A. Colaleo[77a,77b], D. Creanza[77a,77c], N. De Filippis[77a,77c], M. De Palma[77a,77b], W. Elmetenawee[77a,77b,p], N. Ferrara[77a,77c], L. Fiore[77a], L. Generoso[77a,77b], L. Longo[77a], M. Louka[77a,77b], G. Maggi[77a,77c], M. Maggi[77a], I. Margjeka[77a], V. Mastrapasqua[77a,77b], S. My[77a,77b], F. Nenna[77a,77b], S. Nuzzo[77a,77b], A. Pellecchia[77a,77b], A. Pompili[77a,77b], G. Pugliese[77a,77c], R. Radogna[77a,77b], D. Ramos[77a], A. Ranieri[77a], L. Silvestris[77a], F.M. Simone[77a,77c], A. Stamerra[77a,77b], Ü. Sözbilir[77a], D. Troiano[77a,77b], R. Venditti[77a,77b], P. Verwilligen[77a], A. Zaza[77a,77b], G. Abbiendi[78a], C. Battilana[78a,78b], D. Bonacorsi[78a,78b], P. Capiluppi[78a,78b], F.R. Cavallo[78a], M. Cuffiani[78a,78b], T. Diotalevi[78a,78b], F. Fabbri[78a], A. Fanfani[78a,78b], R. Farinelli[78a], D. Fasanella[78a], P. Giacomelli[78a],

2026 JINST 21 P04002

L. Guiducci[78a,78b], S. Lo Meo[78a,as], M. Lorusso[78a,78b], L. Lunerti[78a], S. Marcellini[78a], G. Masetti[78a], F.L. Navarria[78a,78b], G. Paggi[78a,78b], A. Perrotta[78a], A.M. Rossi[78a,78b], S. Rossi Tisbeni[78a,78b], T. Rovelli[78a,78b], G.P. Siroli[78a,78b], S. Costa[79a,79b,at], A. Di Mattia[79a], A. Lapertosa[79a], R. Potenza[79a,79b], A. Tricomi[79a,79b,at], J. Altork[80a,80b], P. Assiouras[80a], G. Barbagli[80a], G. Bardelli[80a], M. Bartolini[80a,80b], A. Calandri[80a,80b], B. Camaiani[80a,80b], A. Cassese[80a], R. Ceccarelli[80a], V. Ciulli[80a,80b], C. Civinini[80a], R. D'Alessandro[80a,80b], L. Damenti[80a,80b], E. Focardi[80a,80b], T. Kello[80a], G. Latino[80a,80b], P. Lenzi[80a,80b], M. Lizzo[80a], M. Meschini[80a], S. Paoletti[80a], A. Papanastassiou[80a,80b], G. Sguazzoni[80a], L. Viliani[80a], L. Benussi[81], S. Colafranceschi[81,au], S. Meola[81,av], D. Piccolo[81], M. Alves Gallo Pereira[82a], F. Ferro[82a], E. Robutti[82a], S. Tosi[82a,82b], A. Benaglia[83a], F. Brivio[83a], V. Camagni[83a,83b], F. Cetorelli[83a,83b], F. De Guio[83a,83b], M.E. Dinardo[83a,83b], P. Dini[83a], S. Gennai[83a], R. Gerosa[83a,83b], A. Ghezzi[83a,83b], P. Govoni[83a,83b], L. Guzzi[83a], M.R. Kim[83a], G. Lavizzari[83a,83b], M.T. Lucchini[83a,83b], M. Malberti[83a], S. Malvezzi[83a], A. Massironi[83a], D. Menasce[83a], L. Moroni[83a], M. Paganoni[83a,83b], S. Palluotto[83a,83b], D. Pedrini[83a], A. Perego[83a,83b], G. Pizzati[83a,83b], T. Tabarelli de Fatis[83a,83b], S. Buontempo[84a], C. Di Fraia[84a,84b], F. Fabozzi[84a,84c], L. Favilla[84a,84d], A.O.M. Iorio[84a,84b], L. Lista[84a,84b,aw], P. Paolucci[84a,ab], B. Rossi[84a], P. Azzi[85a], N. Bacchetta[85a,ax], L. Borella[85a], P. Bortignon[85a,85c], G. Bortolato[85a,85b], A.C.M. Bulla[85a,85c], R. Carlin[85a,85b], P. Checchia[85a], T. Dorigo[85a,ay], F. Gasparini[85a,85b], U. Gasparini[85a,85b], S. Giorgetti[85a], E. Lusiani[85a], M. Margoni[85a,85b], A.T. Meneguzzo[85a,85b], F. Montecassiano[85a], J. Pazzini[85a,85b], F. Primavera[85a,85b], P. Ronchese[85a,85b], R. Rossin[85a,85b], F. Simonetto[85a,85b], M. Tosi[85a,85b], A. Triossi[85a,85b], M. Zanetti[85a,85b], P. Zotto[85a,85b], A. Zucchetta[85a,85b], G. Zumerle[85a,85b], A. Braghieri[86a], M. Brunoldi[86a,86b], S. Calzaferri[86a,86b], P. Montagna[86a,86b], M. Pelliccioni[86a,86b], V. Re[86a], C. Riccardi[86a,86b], P. Salvini[86a], I. Vai[86a,86b], P. Vitulo[86a,86b], S. Ajmal[87a,87b], M.E. Ascioti[87a,87b], G.M. Bilei[87a,†], C. Carrivale[87a,87b], D. Ciangottini[87a,87b], L. Della Penna[87a,87b], L. Fanò[87a,87b], V. Mariani[87a,87b], M. Menichelli[87a], F. Moscatelli[87a,az], A. Rossi[87a,87b], A. Santocchia[87a,87b], D. Spiga[87a], T. Tedeschi[87a,87b], C. Aimè[88a,88b], C.A. Alexe[88a,88c], P. Asenov[88a,88b], P. Azzurri[88a], G. Bagliesi[88a], L. Bianchini[88a,88b], T. Boccali[88a], E. Bossini[88a], D. Bruschini[88a,88c], R. Castaldi[88a], F. Cattafesta[88a,88c], M.A. Ciocci[88a,88d], M. Cipriani[88a,88b], R. Dell'Orso[88a], S. Donato[88a,88b], R. Forti[88a,88b], A. Giassi[88a], F. Ligabue[88a,88c], A.C. Marini[88a,88b], A. Messineo[88a,88b], S. Mishra[88a], V.K. Muraleedharan Nair Bindhu[88a,88b], S. Nandan[88a], F. Palla[88a], M. Riggirello[88a,88c], A. Rizzi[88a,88b], G. Rolandi[88a,88c], S. Roy Chowdhury[88a,ba], T. Sarkar[88a], A. Scribano[88a], P. Solanki[88a,88b], P. Spagnolo[88a], F. Tenchini[88a,88b], R. Tenchini[88a], G. Tonelli[88a,88b], N. Turini[88a,88d], F. Vaselli[88a,88c], A. Venturi[88a], P.G. Verdini[88a], P. Akrap[89a,89b], C. Basile[89a,89b], S.C. Behera[89a], F. Cavallari[89a], L. Cunqueiro Mendez[89a,89b], F. De Riggi[89a,89b], D. Del Re[89a,89b], M. Del Vecchio[89a,89b], E. Di Marco[89a], M. Diemoz[89a], F. Errico[89a], L. Frosina[89a,89b], R. Gargiulo[89a,89b], B. Harikrishnan[89a,89b], F. Lombardi[89a,89b], E. Longo[89a,89b], L. Martikainen[89a,89b], J. Mijuskovic[89a,89b], G. Organtini[89a,89b], N. Palmeri[89a,89b], R. Paramatti[89a,89b], T. Pauletto[89a,89b], S. Rahatlou[89a,89b], C. Rovelli[89a], F. Santanastasio[89a,89b], L. Soffi[89a], V. Vladimirov[89a,89b], N. Amapane[90a,90b], R. Arcidiacono[90a,90c], S. Argiro[90a,90b], M. Arneodo[90a,90c,†], N. Bartosik[90a,90c], R. Bellan[90a,90b], A. Bellora[90a,90b], C. Biino[90a], C. Borca[90a,90b], N. Cartiglia[90a], M. Costa[90a,90b], R. Covarelli[90a,90b], N. Demaria[90a], L. Finco[90a],

2026 JINST 21 P04002

M. Grippo[90a,90b], B. Kiani[90a,90b], L. Lanteri[90a,90b], F. Legger[90a], F. Luongo[90a,90b], C. Mariotti[90a], S. Maselli[90a], A. Mecca[90a,90b], L. Menzio[90a,90b], P. Meridiani[90a], E. Migliore[90a,90b], M. Monteno[90a], M.M. Obertino[90a,90b], G. Ortona[90a], L. Pacher[90a,90b], N. Pastrone[90a], M. Ruspa[90a,90c], F. Siviero[90a,90b], V. Sola[90a,90b], A. Solano[90a,90b], A. Staiano[90a], C. Tarricone[90a,90b], D. Trocino[90a], G. Umoret[90a,90b], E. Vlasov[90a,90b], R. White[90a,90b], J. Babbar[91a,91b,ba], S. Belforte[91a], V. Candelise[91a,91b], M. Casarsa[91a], F. Cossutti[91a], K. De Leo[91a], G. Della Ricca[91a,91b], R. Delli Gatti[91a,91b], S. Dogra[92], J. Hong[92], J. Kim[92], T. Kim[92], D. Lee[92], H. Lee[92], J. Lee[92], S.W. Lee[92], C.S. Moon[92], Y.D. Oh[92], S. Sekmen[92], B. Tae[92], Y.C. Yang[92], M.S. Kim[93], G. Bak[94], P. Gwak[94], H. Kim[94], D.H. Moon[94], J. Seo[94], E. Asilar[95], F. Carnevali[95], J. Choi[95,bb], T.J. Kim[95], Y. Ryou[95], J. Song[95], S. Ha[96], S. Han[96], B. Hong[96], J. Kim[96], K. Lee[96], K.S. Lee[96], S. Lee[96], J. Yoo[96], J. Goh[97], J. Shin[97], S. Yang[97], Y. Kang[98], H. S. Kim[98], Y. Kim[98], B. Ko[98], S. Lee[98], J. Almond[99], J.H. Bhyun[99], J. Choi[99], J. Choi[99], W. Jun[99], H. Kim[99], J. Kim[99], T. Kim[99], Y. Kim[99], Y.W. Kim[99], S. Ko[99], H. Lee[99], J. Lee[99], J. Lee[99], B.H. Oh[99], J. Shin[99], U.K. Yang[99], I. Yoon[99], W. Jang[100], D. Kim[100], S. Kim[100], J.S.H. Lee[100], Y. Lee[100], I.C. Park[100], Y. Roh[100], I.J. Watson[100], G. Cho[101], K. Hwang[101], B. Kim[101], S. Kim[101], K. Lee[101], H.D. Yoo[101], Y. Lee[102], I. Yu[102], T. Beyrouthy[103], Y. Gharbia[103], F. Alazemi[104], K. Dreimanis[105], O.M. Eberlins[105], A. Gaile[105], C. Munoz Diaz[105], D. Osite[105], G. Pikurs[105], R. Plese[105], A. Potrebko[105], M. Seidel[105], D. Sidiropoulos Kontos[105], N.R. Strautnieks[106], M. Ambrozas[107], A. Juodagalvis[107], S. Nargelas[107], A. Rinkevicius[107], G. Tamulaitis[107], I. Yusuff[108,bc], Z. Zolkapli[108], J.F. Benitez[109], A. Castaneda Hernandez[109], A. Cota Rodriguez[109], L.E. Cuevas Picos[109], H.A. Encinas Acosta[109], L.G. Gallegos Maríñez[109], J.A. Murillo Quijada[109], L. Valencia Palomo[109], G. Ayala[110], H. Castilla-Valdez[110], H. Crotte Ledesma[110], R. Lopez-Fernandez[110], J. Mejia Guisao[110], R. Reyes-Almanza[110], A. Sánchez Hernández[110], C. Oropeza Barrera[111], D.L. Ramirez Guadarrama[111], M. Ramírez García[111], I. Bautista[112], F.E. Neri Huerta[112], I. Pedraza[112], H.A. Salazar Ibarguen[112], C. Uribe Estrada[112], I. Bubanja[113], N. Raicevic[113], P.H. Butler[114], A. Ahmad[115], M.I. Asghar[115], A. Awais[115], M.I.M. Awan[115], W.A. Khan[115], V. Avati[116], L. Forthomme[116], L. Grzanka[116], M. Malawski[116], K. Piotrzkowski[116], M. Bluj[117], M. Górski[117], M. Kazana[117], M. Szleper[117], P. Zalewski[117], K. Bunkowski[118], K. Doroba[118], A. Kalinowski[118], M. Konecki[118], J. Krolikowski[118], A. Muhammad[118], P. Fokow[119], K. Pozniak[119], W. Zabolotny[119], M. Araujo[120], D. Bastos[120], C. Beirão Da Cruz E Silva[120], A. Boletti[120], M. Bozzo[120], T. Camporesi[120], G. Da Molin[120], M. Gallinaro[120], J. Hollar[120], N. Leonardo[120], G.B. Marozzo[120], A. Petrilli[120], M. Pisano[120], J. Seixas[120], J. Varela[120], J.W. Wulff[120], P. Adzic[121], L. Markovic[121], P. Milenovic[121], V. Milosevic[121], D. Devetak[122], M. Dordevic[122], J. Milosevic[122], L. Nadderd[122], V. Rekovic[122], M. Stojanovic[122], M. Alcalde Martinez[123], J. Alcaraz Maestre[123], J.A. Brochero Cifuentes[123], M. Cepeda[123], M. Cerrada[123], N. Colino[123], B. De La Cruz[123], A. Delgado Peris[123], A. Escalante Del Valle[123], Cristina F. Bedoya[123], D. Fernández Del Val[123], J.P. Fernández Ramos[123], J. Flix[123], M.C. Fouz[123], M. Gonzalez Hernandez[123], O. Gonzalez Lopez[123], S. Goy Lopez[123], J.M. Hernandez[123], M.I. Josa[123], J. Llorente Merino[123], Oliver M. Carretero[123], C. Martin Perez[123], E. Martin Viscasillas[123], D. Moran[123], C. M. Morcillo Perez[123], Á. Navarro Tobar[123], R. Paz Herrera[123], J. Puerta Pelayo[123], A. Pérez-Calero Yzquierdo[123], I. Redondo[123], J. Vazquez Escobar[123], J.F. de Trocóniz[124], B. Alvarez Gonzalez[125], J. Ayllon Torresano[125],

2026 JINST 21 P04002

A. Cardini[125], J. Cuevas[125], J. Del Riego Badas[125], D. Estrada Acevedo[125], J. Fernandez Menendez[125], S. Folgueras[125], I. Gonzalez Caballero[125], P. Leguina[125], M. Obeso Menendez[125], E. Palencia Cortezon[125], J. Prado Pico[125], A. Soto Rodríguez[125], P. Vischia[125], S. Blanco Fernández[126], I.J. Cabrillo[126], A. Calderon[126], J. Duarte Campderros[126], M. Fernandez[126], G. Gomez[126], C. Lasaosa García[126], R. Lopez Ruiz[126], C. Martinez Rivero[126], P. Martinez Ruiz del Arbol[126], F. Matorras[126], P. Matorras Cuevas[126], E. Navarrete Ramos[126], J. Piedra Gomez[126], C. Quintana San Emeterio[126], L. Scodellaro[126], I. Vila[126], R. Vilar Cortabitarte[126], J.M. Vizan Garcia[126], D.D.C. Wickramarathna[127], B. Kailasapathy[127,bd], W.G.D. Dharmaratna[128,be], K. Liyanage[128], N. Perera[128], D. Abbaneo[129], C. Amendola[129], R. Ardino[129], E. Auffray[129], J. Baechler[129], D. Barney[129], J. Bendavid[129], M. Bianco[129], A. Bocci[129], L. Borgonovi[129], C. Botta[129], A. Bragagnolo[129], C.E. Brown[129], C. Caillol[129], G. Cerminara[129], P. Connor[129], K. Cormier[129], D. d'Enterria[129], A. Dabrowski[129], A. David[129], A. De Roeck[129], M.M. Defranchis[129], M. Deile[129], M. Dobson[129], P.J. Fernández Manteca[129], B.A. Fontana Santos Alves[129], E. Fontanesi[129], W. Funk[129], A. Gaddi[129], S. Giani[129], D. Gigi[129], K. Gill[129], F. Glege[129], M. Glowacki[129], A. Gruber[129], J. Hegeman[129], J.K. Heikkilä[129], R. Hofsaess[129], B. Huber[129], T. James[129], P. Janot[129], O. Kaluzinska[129], O. Karacheban[129,y], G. Karathanasis[129], S. Laurila[129], P. Lecoq[129], E. Leutgeb[129], C. Lourenço[129], A.-M. Lyon[129], M. Magherini[129], L. Malgeri[129], M. Mannelli[129], A. Mehta[129], F. Meijers[129], J.A. Merlin[129], S. Mersi[129], E. Meschi[129], M. Migliorini[129], F. Monti[129], F. Moortgat[129], M. Mulders[129], M. Musich[129], I. Neutelings[129], S. Orfanelli[129], F. Pantaleo[129], M. Pari[129], G. Petrucciani[129], A. Pfeiffer[129], M. Pierini[129], M. Pitt[129], H. Qu[129], D. Rabady[129], A. Reimers[129], B. Ribeiro Lopes[129], F. Riti[129], P. Rosado[129], M. Rovere[129], H. Sakulin[129], R. Salvatico[129], S. Sanchez Cruz[129], S. Scarfi[129], M. Selvaggi[129], K. Shchelina[129], P. Silva[129], P. Sphicas[129,bf], A.G. Stahl Leiton[129], A. Steen[129], S. Summers[129], D. Treille[129], P. Tropea[129], E. Vernazza[129], J. Wanczyk[129,bg], S. Wuchterl[129], M. Zarucki[129], P. Zehetner[129], P. Zejdl[129], G. Zevi Della Porta[129], L. Caminada[130,bh], W. Erdmann[130], R. Horisberger[130], Q. Ingram[130], H.C. Kaestli[130], D. Kotlinski[130], C. Lange[130], U. Langenegger[130], A. Nigamova[130], L. Noehte[130,bh], T. Rohe[130], A. Samalan[130], T.K. Aarrestad[131], M. Backhaus[131], T. Bevilacqua[131,bh], G. Bonomelli[131], C. Cazzaniga[131], K. Datta[131], P. De Bryas Dexmiers D'Archiacchiac[131,bg], A. De Cosa[131], G. Dissertori[131], M. Dittmar[131], M. Donegà[131], F. Glessgen[131], C. Grab[131], T.G. Harte[131], N. Härringer[131], W. Lustermann[131], M. Malucchi[131], R.A. Manzoni[131], L. Marchese[131], A. Mascellani[131,bg], F. Nessi-Tedaldi[131], F. Pauss[131], B. Ristic[131], R. Seidita[131], J. Steggemann[131,bg], A. Tarabini[131], D. Valsecchi[131], R. Wallny[131], C. Amsler[132,bi], F. Bilandzija[132], P. Bärtschi[132], M.F. Canelli[132], G. Celotto[132], V. Guglielmi[132], A. Jofrehei[132], B. Kilminster[132], T.H. Kwok[132], S. Leontsinis[132], V. Lukashenko[132], A. Macchiolo[132], F. Meng[132], M. Missiroli[132], J. Motta[132], P. Robmann[132], E. Shokr[132], F. Stäger[132], R. Tramontano[132], P. Viscone[132], D. Bhowmik[133], C.M. Kuo[133], P.K. Rout[133], S. Taj[133], P.C. Tiwari[133,ak], L. Ceard[134], K.F. Chen[134], Z.g. Chen[134], A. De Iorio[134], W.-S. Hou[134], T.h. Hsu[134], Y.w. Kao[134], S. Karmakar[134], G. Kole[134], Y.y. Li[134], R.-S. Lu[134], E. Paganis[134], X.f. Su[134], J. Thomas-Wilsker[134], L.s. Tsai[134], D. Tsionou[134], H.y. Wu[134], E. Yazgan[134], C. Asawatangtrakuldee[135], N. Srimanobhas[135], Y. Maghrbi[136], D. Agyel[137], F. Dolek[137], I. Dumanoglu[137,bj], Y. Guler[137,bk], E. Gurpinar Guler[137,bk], C. Isik[137], O. Kara[137,bl], A. Kayis Topaksu[137], Y. Komurcu[137], G. Onengut[137], K. Ozdemir[137,bm],

2026 JINST 21 P04002

B. Tali[137,bn], U.G. Tok[137], E. Uslan[137], I.S. Zorbakir[137], S. Sen[138], M. Yalvac[139,bo], B. Akgun[140], I.O. Atakisi[140,bp], E. Gülmez[140], M. Kaya[140,bq], O. Kaya[140,br], M.A. Sarkisla[140,bs], S. Tekten[140,bt], D. Boncukcu[141], A. Cakir[141], K. Cankocak[141,bj,bu], B. Hacisahinoglu[142], I. Hos[142,bv], B. Kaynak[142], S. Ozkorucuklu[142], O. Potok[142], H. Sert[142], C. Simsek[142], C. Zorbilmez[142], S. Cerci[143], C. Dozen[143,bw], B. Isildak[143], E. Simsek[143], D. Sunar Cerci[143], T. Yetkin[143,bw], A. Boyaryntsev[144], O. Dadazhanova[144], B. Grynyov[144], L. Levchuk[145], J.J. Brooke[146], A. Bundock[146], F. Bury[146], E. Clement[146], D. Cussans[146], D. Dharmender[146], H. Flacher[146], J. Goldstein[146], H.F. Heath[146], M.-L. Holmberg[146], L. Kreczko[146], S. Paramesvaran[146], L. Robertshaw[146], M.S. Sanjrani[146,an], J. Segal[146], V.J. Smith[146], A.H. Ball[147], K.W. Bell[147], A. Belyaev[147,bx], C. Brew[147], R.M. Brown[147], D.J.A. Cockerill[147], A. Elliot[147], K.V. Ellis[147], J. Gajownik[147], K. Harder[147], S. Harper[147], J. Linacre[147], K. Manolopoulos[147], M. Moallemi[147], D.M. Newbold[147], E. Olaiya[147], D. Petyt[147], T. Reis[147], A.R. Sahasransu[147], G. Salvi[147], T. Schuh[147], C.H. Shepherd-Themistocleous[147], I.R. Tomalin[147], K.C. Whalen[147], T. Williams[147], I. Andreou[148], R. Bainbridge[148], P. Bloch[148], O. Buchmuller[148], C.A. Carrillo Montoya[148], D. Colling[148], I. Das[148], P. Dauncey[148], G. Davies[148], M. Della Negra[148], S. Fayer[148], G. Fedi[148], G. Hall[148], H.R. Hoorani[148], A. Howard[148], G. Iles[148], C.R. Knight[148], P. Krueper[148], J. Langford[148], K.H. Law[148], J. León Holgado[148], L. Lyons[148], A.-M. Magnan[148], B. Maier[148], S. Mallios[148], A. Mastronikolis[148], M. Mieskolainen[148], J. Nash[148,by], M. Pesaresi[148], P.B. Pradeep[148], B.C. Radburn-Smith[148], A. Richards[148], A. Rose[148], L. Russell[148], K. Savva[148], R. Schmitz[148], C. Seez[148], R. Shukla[148], A. Tapper[148], K. Uchida[148], G.P. Uttley[148], T. Virdee[148,ab], M. Vojinovic[148], N. Wardle[148], D. Winterbottom[148], J.E. Cole[149], A. Khan[149], P. Kyberd[149], I.D. Reid[149], S. Abdullin[150], A. Brinkerhoff[150], E. Collins[150], M.R. Darwish[150], J. Dittmann[150], K. Hatakeyama[150], V. Hegde[150], J. Hiltbrand[150], B. McMaster[150], J. Samudio[150], S. Sawant[150], C. Sutantawibul[150], J. Wilson[150], J.M. Hogan[151], R. Bartek[152], A. Dominguez[152], S. Raj[152], B. Sahu[152], A.E. Simsek[152], S.S. Yu[152], B. Bam[153], A. Buchot Perraguin[153], S. Campbell[153], R. Chudasama[153], S.I. Cooper[153], C. Crovella[153], G. Fidalgo[153], S.V. Gleyzer[153], A. Khukhunaishvili[153], K. Matchev[153], E. Pearson[153], P. Rumerio[153,bz], E. Usai[153], R. Yi[153], S. Cholak[154], G. De Castro[154], Z. Demiragli[154], C. Erice[154], C. Fangmeier[154], C. Fernandez Madrazo[154], J. Fulcher[154], F. Golf[154], S. Jeon[154], J. O'Cain[154], I. Reed[154], J. Rohlf[154], K. Salyer[154], D. Sperka[154], D. Spitzbart[154], I. Suarez[154], A. Tsatsos[154], E. Wurtz[154], A.G. Zecchinelli[154], G. Barone[155], G. Benelli[155], D. Cutts[155], S. Ellis[155], L. Gouskos[155], M. Hadley[155], U. Heintz[155], K.W. Ho[155], T. Kwon[155], L. Lambrecht[155], G. Landsberg[155], K.T. Lau[155], J. Luo[155], S. Mondal[155], J. Roloff[155], T. Russell[155], S. Sagir[155,ca], X. Shen[155], M. Stamenkovic[155], N. Venkatasubramanian[155], S. Abbott[156], S. Baradia[156], B. Barton[156], R. Breedon[156], H. Cai[156], M. Calderon De La Barca Sanchez[156], E. Cannaert[156], M. Chertok[156], M. Citron[156], J. Conway[156], P.T. Cox[156], F. Eble[156], R. Erbacher[156], O. Kukral[156], G. Mocellin[156], S. Ostrom[156], I. Salazar Segovia[156], J.S. Tafoya Vargas[156], W. Wei[156], S. Yoo[156], K. Adamidis[157], M. Bachtis[157], D. Campos[157], R. Cousins[157], S. Crossley[157], G. Flores Avila[157], J. Hauser[157], M. Ignatenko[157], M.A. Iqbal[157], T. Lam[157], Y.f. Lo[157], E. Manca[157], A. Nunez Del Prado[157], D. Saltzberg[157], V. Valuev[157], R. Clare[158], J.W. Gary[158], G. Hanson[158], A. Aportela[159], A. Arora[159], J.G. Branson[159], S. Cittolin[159], S. Cooperstein[159], B. D'Anzi[159], D. Diaz[159], J. Duarte[159], L. Giannini[159], Y. Gu[159], J. Guiang[159], V. Krutelyov[159], R. Lee[159],

2026 JINST 21 P04002

J. Letts[159], H. Li[159], M. Masciovecchio[159], F. Mokhtar[159], S. Mukherjee[159], M. Pieri[159], D. Primosch[159], M. Quinnan[159], V. Sharma[159], M. Tadel[159], E. Vourliotis[159], F. Würthwein[159], A. Yagil[159], Z. Zhao[159], A. Barzdukas[160], L. Brennan[160], C. Campagnari[160], S. Carron Montero[160,cb], K. Downham[160], C. Grieco[160], M.M. Hussain[160], J. Incandela[160], M.W.K. Lai[160], A.J. Li[160], P. Masterson[160], J. Richman[160], S.N. Santpur[160], D. Stuart[160], T.Á. Vámi[160], X. Yan[160], D. Zhang[160], A. Albert[161], S. Bhattacharya[161], A. Bornheim[161], O. Cerri[161], R. Kansal[161], H.B. Newman[161], G. Reales Gutiérrez[161], T. Sievert[161], M. Spiropulu[161], J.R. Vlimant[161], R.A. Wynne[161], S. Xie[161], J. Alison[162], S. An[162], M. Cremonesi[162], V. Dutta[162], E.Y. Ertorer[162], T. Ferguson[162], T.A. Gómez Espinosa[162], A. Harilal[162], A. Kallil Tharayil[162], M. Kanemura[162], C. Liu[162], M. Marchegiani[162], P. Meiring[162], S. Murthy[162], P. Palit[162], K. Park[162], M. Paulini[162], A. Roberts[162], A. Sanchez[162], W. Terrill[162], J.P. Cumalat[163], W.T. Ford[163], A. Hart[163], S. Kwan[163], J. Pearkes[163], C. Savard[163], N. Schonbeck[163], K. Stenson[163], K.A. Ulmer[163], S.R. Wagner[163], N. Zipper[163], D. Zuolo[163], J. Alexander[164], X. Chen[164], J. Dickinson[164], A. Duquette[164], J. Fan[164], X. Fan[164], J. Grassi[164], S. Hogan[164], P. Kotamnives[164], J. Monroy[164], G. Niendorf[164], M. Oshiro[164], J.R. Patterson[164], A. Ryd[164], J. Thom[164], P. Wittich[164], R. Zou[164], L. Zygala[164], M. Albrow[165], M. Alyari[165], O. Amram[165], G. Apollinari[165], A. Apresyan[165], L.A.T. Bauerdick[165], D. Berry[165], J. Berryhill[165], P.C. Bhat[165], K. Burkett[165], J.N. Butler[165], A. Canepa[165], G.B. Cerati[165], H.W.K. Cheung[165], F. Chlebana[165], C. Cosby[165], G. Cummings[165], I. Dutta[165], V.D. Elvira[165], J. Freeman[165], A. Gandrakota[165], Z. Gecse[165], L. Gray[165], D. Green[165], A. Grummer[165], S. Grünendahl[165], D. Guerrero[165], O. Gutsche[165], R.M. Harris[165], J. Hirschauer[165], V. Innocente[165], B. Jayatilaka[165], S. Jindariani[165], M. Johnson[165], U. Joshi[165], R.S. Kim[165], B. Klima[165], S. Lammel[165], D. Lincoln[165], R. Lipton[165], T. Liu[165], K. Maeshima[165], D. Mason[165], P. McBride[165], P. Merkel[165], S. Mrenna[165], S. Nahn[165], J. Ngadiuba[165], D. Noonan[165], S. Norberg[165], V. Papadimitriou[165], N. Pastika[165], K. Pedro[165], C. Pena[165,cc], C.E. Perez Lara[165], V. Perovic[165], F. Ravera[165], A. Reinsvold Hall[165,cd], L. Ristori[165], M. Safdari[165], E. Sexton-Kennedy[165], E. Smith[165], N. Smith[165], A. Soha[165], L. Spiegel[165], S. Stoynev[165], J. Strait[165], L. Taylor[165], S. Tkaczyk[165], N.V. Tran[165], L. Uplegger[165], E.W. Vaandering[165], C. Wang[165], I. Zoi[165], C. Aruta[166], P. Avery[166], D. Bourilkov[166], P. Chang[166], V. Cherepanov[166], R.D. Field[166], C. Huh[166], E. Koenig[166], M. Kolosova[166], J. Konigsberg[166], A. Korytov[166], G. Mitselmakher[166], K. Mohrman[166], A. Muthirakalayil Madhu[166], N. Rawal[166], S. Rosenzweig[166], V. Sulimov[166], Y. Takahashi[166], J. Wang[166], T. Adams[167], A. Al Kadhim[167], A. Askew[167], S. Bower[167], R. Goff[167], R. Hashmi[167], A. Hassani[167], T. Kolberg[167], G. Martinez[167], M. Mazza[167], H. Prosper[167], P.R. Prova[167], R. Yohay[167], B. Alsufyani[168], S. Butalla[168], S. Das[168], M. Hohlmann[168], M. Lavinsky[168], E. Yanes[168], M.R. Adams[169], N. Barnett[169], A. Baty[169], C. Bennett[169], R. Cavanaugh[169], R. Escobar Franco[169], O. Evdokimov[169], C.E. Gerber[169], H. Gupta[169], M. Hawksworth[169], A. Hingrajiya[169], D.J. Hofman[169], Z. Huang[169], J.h. Lee[169], C. Mills[169], S. Nanda[169], G. Nigmatkulov[169], B. Ozek[169], T. Phan[169], D. Pilipovic[169], R. Pradhan[169], E. Prifti[169], P. Roy[169], T. Roy[169], D. Shekar[169], N. Singh[169], A. Thielen[169], M.B. Tonjes[169], N. Varelas[169], M.A. Wadud[169], J. Yoo[169], M. Alhusseini[170], D. Blend[170], K. Dilsiz[170,ce], O.K. Köseyan[170], A. Mestvirishvili[170,cf], O. Neogi[170], H. Ogul[170,cg], Y. Onel[170], A. Penzo[170], C. Snyder[170], E. Tiras[170,ch], B. Blumenfeld[171], J. Davis[171], A.V. Gritsan[171], L. Kang[171], S. Kyriacou[171], P. Maksimovic[171], M. Roguljic[171], S. Sekhar[171], M.V. Srivastav[171],

2026 JINST 21 P04002

M. Swartz[171], A. Abreu[172], L.F. Alcerro Alcerro[172], J. Anguiano[172], S. Arteaga Escatel[172], P. Baringer[172], A. Bean[172], R. Bhattacharya[172], Z. Flowers[172], D. Grove[172], J. King[172], G. Krintiras[172], M. Lazarovits[172], C. Le Mahieu[172], J. Marquez[172], M. Murray[172], M. Nickel[172], S. Popescu[172,ci], C. Rogan[172], C. Royon[172], S. Rudrabhatla[172], S. Sanders[172], C. Smith[172], G. Wilson[172], B. Allmond[173], N. Islam[173], A. Ivanov[173], K. Kaadze[173], Y. Maravin[173], J. Natoli[173], G.G. Reddy[173], D. Roy[173], G. Sorrentino[173], A. Baden[174], A. Belloni[174], J. Bistany-riebman[174], S.C. Eno[174], N.J. Hadley[174], S. Jabeen[174], R.G. Kellogg[174], T. Koeth[174], B. Kronheim[174], S. Lascio[174], P. Major[174], A.C. Mignerey[174], C. Palmer[174], C. Papageorgakis[174], M.M. Paranjpe[174], E. Popova[174,cj], A. Shevelev[174], L. Zhang[174], C. Baldenegro Barrera[175], H. Bossi[175], S. Bright-Thonney[175], I.A. Cali[175], Y.c. Chen[175], P.c. Chou[175], M. D'Alfonso[175], J. Eysermans[175], C. Freer[175], G. Gomez-Ceballos[175], M. Goncharov[175], G. Grosso[175], P. Harris[175], D. Hoang[175], G.M. Innocenti[175], K. Ivanov[175], G. Kopp[175], D. Kovalskyi[175], L. Lavezzo[175], Y.-J. Lee[175], K. Long[175], C. Mcginn[175], A. Novak[175], M.I. Park[175], C. Paus[175], C. Reissel[175], C. Roland[175], G. Roland[175], S. Rothman[175], T.a. Sheng[175], G.S.F. Stephans[175], D. Walter[175], J. Wang[175], Z. Wang[175], B. Wyslouch[175], T. J. Yang[175], A. Alpana[176], B. Crossman[176], W.J. Jackson[176], C. Kapsiak[176], M. Krohn[176], D. Mahon[176], J. Mans[176], B. Marzocchi[176], R. Rusack[176], O. Sancar[176], R. Saradhy[176], N. Strobbe[176], K. Bloom[177], D.R. Claes[177], G. Haza[177], J. Hossain[177], C. Joo[177], I. Kravchenko[177], K.H.M. Kwok[177], A. Rohilla[177], J.E. Siado[177], W. Tabb[177], A. Vagnerini[177], A. Wightman[177], H. Bandyopadhyay[178], L. Hay[178], H.w. Hsia[178], I. Iashvili[178], A. Kalogeropoulos[178], A. Kharchilava[178], A. Mandal[178], M. Morris[178], D. Nguyen[178], S. Rappoccio[178], H. Rejeb Sfar[178], A. Williams[178], D. Yu[178], A. Aarif[179], G. Alverson[179], E. Barberis[179], J. Bonilla[179], B. Bylsma[179], M. Campana[179], J. Dervan[179], Y. Haddad[179], Y. Han[179], I. Israr[179], A. Krishna[179], M. Lu[179], N. Manganelli[179], R. Mccarthy[179], D.M. Morse[179], T. Orimoto[179], L. Skinnari[179], C.S. Thoreson[179], E. Tsai[179], D. Wood[179], S. Dittmer[180], K.A. Hahn[180], M. Mcginnis[180], Y. Miao[180], D.G. Monk[180], M.H. Schmitt[180], A. Taliercio[180], M. Velasco[180], J. Wang[180], G. Agarwal[181], R. Band[181], R. Bucci[181], S. Castells[181], A. Das[181], A. Datta[181], A. Ehnis[181], R. Goldouzian[181], M. Hildreth[181], K. Hurtado Anampa[181], T. Ivanov[181], C. Jessop[181], A. Karneyeu[181], K. Lannon[181], J. Lawrence[181], N. Loukas[181], L. Lutton[181], J. Mariano[181], N. Marinelli[181], T. McCauley[181], C. Mcgrady[181], C. Moore[181], Y. Musienko[181,ck], H. Nelson[181], M. Osherson[181], A. Piccinelli[181], R. Ruchti[181], A. Townsend[181], Y. Wan[181], M. Wayne[181], H. Yockey[181], M. Carrigan[182], R. De Los Santos[182], L.S. Durkin[182], C. Hill[182], M. Joyce[182], D.A. Wenzl[182], B.L. Winer[182], B. R. Yates[182], H. Bouchamaoui[183], G. Dezoort[183], P. Elmer[183], A. Frankenthal[183], M. Galli[183], B. Greenberg[183], N. Haubrich[183], K. Kennedy[183], Y. Lai[183], D. Lange[183], A. Loeliger[183], D. Marlow[183], I. Ojalvo[183], J. Olsen[183], F. Simpson[183], D. Stickland[183], C. Tully[183], S. Malik[184], R. Sharma[184], S. Chandra[185], A. Gu[185], L. Gutay[185], M. Huwiler[185], M. Jones[185], A.W. Jung[185], D. Kondratyev[185], J. Li[185], M. Liu[185], G. Negro[185], N. Neumeister[185], G. Paspalaki[185], S. Piperov[185], N.R. Saha[185], J.F. Schulte[185], F. Wang[185], A. Wildridge[185], W. Xie[185], Y. Yao[185], Y. Zhong[185], N. Parashar[186], A. Pathak[186], E. Shumka[186], D. Acosta[187], A. Agrawal[187], C. Arbour[187], T. Carnahan[187], P. Das[187], K.M. Ecklund[187], F.J.M. Geurts[187], T. Huang[187], I. Krommydas[187], N. Lewis[187], W. Li[187], J. Lin[187], O. Miguel Colin[187], B.P. Padley[187], R. Redjimi[187], J. Rotter[187], C. Vico Villalba[187], M. Wulansatiti[187], E. Yigitbasi[187], Y. Zhang[187], O. Bessidskaia Bylund[188], A. Bodek[188], P. de Barbaro[188,†],

2026 JINST 21 P04002

R. Demina[188], A. Garcia-Bellido[188], H.S. Hare[188], O. Hindrichs[188], N. Parmar[188], P. Parygin[188,cj], H. Seo[188], R. Taus[188], Y.h. Yu[188], B. Chiarito[189], J.P. Chou[189], S.V. Clark[189], S. Donnelly[189], D. Gadkari[189], Y. Gershtein[189], E. Halkiadakis[189], C. Houghton[189], D. Jaroslawski[189], A. Kobert[189], I. Laflotte[189], A. Lath[189], J. Martins[189], M. Perez Prada[189], B. Rand[189], J. Reichert[189], P. Saha[189], S. Salur[189], S. Somalwar[189], R. Stone[189], S.A. Thayil[189], S. Thomas[189], J. Vora[189], D. Ally[190], A.G. Delannoy[190], S. Fiorendi[190], J. Harris[190], T. Holmes[190], A.R. Kanuganti[190], N. Karunarathna[190], J. Lawless[190], L. Lee[190], E. Nibigira[190], B. Skipworth[190], S. Spanier[190], D. Aebi[191], M. Ahmad[191], T. Akhter[191], K. Androsov[191], A. Basnet[191], A. Bolshov[191], O. Bouhali[191,cl], A. Cagnotta[191], V. D'Amante[191], R. Eusebi[191], P. Flanagan[191], J. Gilmore[191], Y. Guo[191], T. Kamon[191], S. Luo[191], R. Mueller[191], A. Safonov[191], N. Akchurin[192], J. Damgov[192], Y. Feng[192], N. Gogate[192], W. Jin[192], S.W. Lee[192], C. Madrid[192], A. Mankel[192], T. Peltola[192], I. Volobouev[192], E. Appelt[193], Y. Chen[193], S. Greene[193], A. Gurrola[193], W. Johns[193], R. Kunnawalkam Elayavalli[193], A. Melo[193], D. Rathjens[193], F. Romeo[193], P. Sheldon[193], S. Tuo[193], J. Velkovska[193], J. Viinikainen[193], J. Zhang[193], B. Cardwell[194], H. Chung[194], B. Cox[194], J. Hakala[194], G. Hamilton Ilha Machado[194], R. Hirosky[194], M. Jose[194], A. Ledovskoy[194], C. Mantilla[194], C. Neu[194], C. Ramón Álvarez[194], Z. Wu[194], S. Bhattacharya[195], P.E. Karchin[195], A. Aravind[196], S. Banerjee[196], K. Black[196], T. Bose[196], E. Chavez[196], S. Dasu[196], P. Everaerts[196], C. Galloni[196], H. He[196], M. Herndon[196], A. Herve[196], C.K. Koraka[196], S. Lomte[196], R. Loveless[196], A. Mallampalli[196], A. Mohammadi[196], S. Mondal[196], T. Nelson[196], G. Parida[196], D. Pinna[196], L. Pétré[196], A. Savin[196], V. Shang[196], V. Sharma[196], W.H. Smith[196], D. Teague[196], A. Warden[196], S. Afanasiev[197], V. Alexakhin[197], Yu. Andreev[197], T. Aushev[197], D. Budkouski[197], R. Chistov[197], M. Danilov[197], T. Dimova[197], A. Ershov[197], S. Gninenko[197], I. Gorbunov[197], A. Kamenev[197], V. Karjavine[197], M. Kirsanov[197], V. Klyukhin[197], O. Kodolova[197,cm], V. Korenkov[197], I. Korsakov[197], A. Kozyrev[197], N. Krasnikov[197], A. Lanev[197], A. Malakhov[197], V. Matveev[197], A. Nikitenko[197,cn,co], V. Palichik[197], V. Perelygin[197], S. Petrushanko[197], O. Radchenko[197], M. Savina[197], V. Shalaev[197], S. Shmatov[197], S. Shulha[197], Y. Skovpen[197], K. Slizhevskiy[197], V. Smirnov[197], O. Teryaev[197], I. Tlisova[197], A. Toropin[197], N. Voytishin[197], A. Zarubin[197], I. Zhizhin[197], E. Boos[198], V. Bunichev[198], M. Dubinin[198,cc], L. Dudko[198], A. Gribushin[198], V. Kim[198,ck], V. Murzin[198], V. Oreshkin[198], V. Savrin[198], A. Snigirev[198], D. Sosnov[198]

[1] *Yerevan Physics Institute, Yerevan, Armenia*
[2] *Institut für Hochenergiephysik, Vienna, Austria*
[3] *Universiteit Antwerpen, Antwerpen, Belgium*
[4] *Vrije Universiteit Brussel, Brussel, Belgium*
[5] *Université Libre de Bruxelles, Bruxelles, Belgium*
[6] *Ghent University, Ghent, Belgium*
[7] *Université Catholique de Louvain, Louvain-la-Neuve, Belgium*
[8] *Centro Brasileiro de Pesquisas Fisicas, Rio de Janeiro, Brazil*
[9] *Universidade do Estado do Rio de Janeiro, Rio de Janeiro, Brazil*
[10] *Universidade Estadual Paulista, Universidade Federal do ABC, São Paulo, Brazil*
[11] *Institute for Nuclear Research and Nuclear Energy, Bulgarian Academy of Sciences, Sofia, Bulgaria*
[12] *University of Sofia, Sofia, Bulgaria*
[13] *Instituto De Alta Investigación, Universidad de Tarapacá, Casilla 7 D, Arica, Chile*
[14] *Universidad Tecnica Federico Santa Maria, Valparaiso, Chile*
[15] *Beihang University, Beijing, China*
[16] *Department of Physics, Tsinghua University, Beijing, China*

2026 JINST 21 P04002

[17] *Institute of High Energy Physics, Beijing, China*
[18] *State Key Laboratory of Nuclear Physics and Technology, Peking University, Beijing, China*
[19] *State Key Laboratory of Nuclear Physics and Technology, Institute of Quantum Matter, South China Normal University, Guangzhou, China*
[20] *Sun Yat-Sen University, Guangzhou, China*
[21] *University of Science and Technology of China, Hefei, China*
[22] *Nanjing Normal University, Nanjing, China*
[23] *Institute of Modern Physics and Key Laboratory of Nuclear Physics and Ion-beam Application (MOE) — Fudan University, Shanghai, China*
[24] *Zhejiang University, Hangzhou, Zhejiang, China*
[25] *Universidad de Los Andes, Bogota, Colombia*
[26] *Universidad de Antioquia, Medellin, Colombia*
[27] *University of Split, Faculty of Electrical Engineering, Mechanical Engineering and Naval Architecture, Split, Croatia*
[28] *University of Split, Faculty of Science, Split, Croatia*
[29] *Institute Rudjer Boskovic, Zagreb, Croatia*
[30] *University of Cyprus, Nicosia, Cyprus*
[31] *Charles University, Prague, Czech Republic*
[32] *Universidad San Francisco de Quito, Quito, Ecuador*
[33] *Academy of Scientific Research and Technology of the Arab Republic of Egypt, Egyptian Network of High Energy Physics, Cairo, Egypt*
[34] *Center for High Energy Physics (CHEP-FU), Fayoum University, El-Fayoum, Egypt*
[35] *National Institute of Chemical Physics and Biophysics, Tallinn, Estonia*
[36] *Department of Physics, University of Helsinki, Helsinki, Finland*
[37] *Helsinki Institute of Physics, Helsinki, Finland*
[38] *Lappeenranta-Lahti University of Technology, Lappeenranta, Finland*
[39] *IRFU, CEA, Université Paris-Saclay, Gif-sur-Yvette, France*
[40] *Laboratoire Leprince-Ringuet, CNRS/IN2P3, Ecole Polytechnique, Institut Polytechnique de Paris, Palaiseau, France*
[41] *Université de Strasbourg, CNRS, IPHC UMR 7178, Strasbourg, France*
[42] *Centre de Calcul de l'Institut National de Physique Nucleaire et de Physique des Particules, CNRS/IN2P3, Villeurbanne, France*
[43] *Institut de Physique des 2 Infinis de Lyon (IP2I), Villeurbanne, France*
[44] *Georgian Technical University, Tbilisi, Georgia*
[45] *RWTH Aachen University, I. Physikalisches Institut, Aachen, Germany*
[46] *RWTH Aachen University, III. Physikalisches Institut A, Aachen, Germany*
[47] *RWTH Aachen University, III. Physikalisches Institut B, Aachen, Germany*
[48] *Deutsches Elektronen-Synchrotron, Hamburg, Germany*
[49] *University of Hamburg, Hamburg, Germany*
[50] *Karlsruher Institut fuer Technologie, Karlsruhe, Germany*
[51] *Institute of Nuclear and Particle Physics (INPP), NCSR Demokritos, Aghia Paraskevi, Greece*
[52] *National and Kapodistrian University of Athens, Athens, Greece*
[53] *National Technical University of Athens, Athens, Greece*
[54] *University of Ioánnina, Ioánnina, Greece*
[55] *HUN-REN Wigner Research Centre for Physics, Budapest, Hungary*
[56] *MTA-ELTE Lendület CMS Particle and Nuclear Physics Group, Eötvös Loránd University, Budapest, Hungary*
[57] *Faculty of Informatics, University of Debrecen, Debrecen, Hungary*
[58] *HUN-REN ATOMKI — Institute of Nuclear Research, Debrecen, Hungary*
[59] *Karoly Robert Campus, MATE Institute of Technology, Gyongyos, Hungary*
[60] *IIT Bhubaneswar, Bhubaneswar, India*
[61] *Panjab University, Chandigarh, India*
[62] *University of Delhi, Delhi, India*
[63] *Indian Institute of Technology Mandi (IIT-Mandi), Himachal Pradesh, India*
[64] *University of Hyderabad, Hyderabad, India*
[65] *Indian Institute of Technology Kanpur, Kanpur, India*

2026 JINST 21 P04002

[66] *Saha Institute of Nuclear Physics, HBNI, Kolkata, India*
[67] *Indian Institute of Technology Madras, Madras, India*
[68] *IISER Mohali, India, Mohali, India*
[69] *Tata Institute of Fundamental Research-A, Mumbai, India*
[70] *Tata Institute of Fundamental Research-B, Mumbai, India*
[71] *National Institute of Science Education and Research, An OCC of Homi Bhabha National Institute, Bhubaneswar, Odisha, India*
[72] *Indian Institute of Science Education and Research (IISER), Pune, India*
[73] *Indian Institute of Technology Hyderabad, Telangana, India*
[74] *Isfahan University of Technology, Isfahan, Iran*
[75] *Institute for Research in Fundamental Sciences (IPM), Tehran, Iran*
[76] *University College Dublin, Dublin, Ireland*
[77a] *INFN Sezione di Bari, Bari, Italy*
[77b] *Università di Bari, Bari, Italy*
[77c] *Politecnico di Bari, Bari, Italy*
[78a] *INFN Sezione di Bologna, Bologna, Italy*
[78b] *Università di Bologna, Bologna, Italy*
[79a] *INFN Sezione di Catania, Catania, Italy*
[79b] *Università di Catania, Catania, Italy*
[80a] *INFN Sezione di Firenze, Firenze, Italy*
[80b] *Università di Firenze, Firenze, Italy*
[81] *INFN Laboratori Nazionali di Frascati, Frascati, Italy*
[82a] *INFN Sezione di Genova, Genova, Italy*
[82b] *Università di Genova, Genova, Italy*
[83a] *INFN Sezione di Milano-Bicocca, Milano, Italy*
[83b] *Università di Milano-Bicocca, Milano, Italy*
[84a] *INFN Sezione di Napoli, Napoli, Italy*
[84b] *Università di Napoli 'Federico II', Napoli, Italy*
[84c] *Università della Basilicata, Potenza, Italy*
[84d] *Scuola Superiore Meridionale (SSM), Napoli, Italy*
[85a] *INFN Sezione di Padova, Padova, Italy*
[85b] *Università di Padova, Padova, Italy*
[85c] *Universita degli Studi di Cagliari, Cagliari, Italy*
[86a] *INFN Sezione di Pavia, Pavia, Italy*
[86b] *Università di Pavia, Pavia, Italy*
[87a] *INFN Sezione di Perugia, Perugia, Italy*
[87b] *Università di Perugia, Perugia, Italy*
[88a] *INFN Sezione di Pisa, Pisa, Italy*
[88b] *Università di Pisa, Pisa, Italy*
[88c] *Scuola Normale Superiore di Pisa, Pisa, Italy*
[88d] *Università di Siena, Siena, Italy*
[89a] *INFN Sezione di Roma, Roma, Italy*
[89b] *Sapienza Università di Roma, Roma, Italy*
[90a] *INFN Sezione di Torino, Torino, Italy*
[90b] *Università di Torino, Torino, Italy*
[90c] *Università del Piemonte Orientale, Novara, Italy*
[91a] *INFN Sezione di Trieste, Trieste, Italy*
[91b] *Università di Trieste, Trieste, Italy*
[92] *Kyungpook National University, Daegu, Korea*
[93] *Department of Mathematics and Physics — GWNU, Gangneung, Korea*
[94] *Chonnam National University, Institute for Universe and Elementary Particles, Kwangju, Korea*
[95] *Hanyang University, Seoul, Korea*
[96] *Korea University, Seoul, Korea*

2026 JINST 21 P04002

[97] *Kyung Hee University, Department of Physics, Seoul, Korea*
[98] *Sejong University, Seoul, Korea*
[99] *Seoul National University, Seoul, Korea*
[100] *University of Seoul, Seoul, Korea*
[101] *Yonsei University, Department of Physics, Seoul, Korea*
[102] *Sungkyunkwan University, Suwon, Korea*
[103] *College of Engineering and Technology, American University of the Middle East (AUM), Dasman, Kuwait*
[104] *Kuwait University — College of Science — Department of Physics, Safat, Kuwait*
[105] *Riga Technical University, Riga, Latvia*
[106] *University of Latvia (LU), Riga, Latvia*
[107] *Vilnius University, Vilnius, Lithuania*
[108] *National Centre for Particle Physics, Universiti Malaya, Kuala Lumpur, Malaysia*
[109] *Universidad de Sonora (UNISON), Hermosillo, Mexico*
[110] *Centro de Investigacion y de Estudios Avanzados del IPN, Mexico City, Mexico*
[111] *Universidad Iberoamericana, Mexico City, Mexico*
[112] *Benemerita Universidad Autonoma de Puebla, Puebla, Mexico*
[113] *University of Montenegro, Podgorica, Montenegro*
[114] *University of Canterbury, Christchurch, New Zealand*
[115] *National Centre for Physics, Quaid-I-Azam University, Islamabad, Pakistan*
[116] *AGH University of Krakow, Krakow, Poland*
[117] *National Centre for Nuclear Research, Swierk, Poland*
[118] *Institute of Experimental Physics, Faculty of Physics, University of Warsaw, Warsaw, Poland*
[119] *Warsaw University of Technology, Warsaw, Poland*
[120] *Laboratório de Instrumentação e Física Experimental de Partículas, Lisboa, Portugal*
[121] *Faculty of Physics, University of Belgrade, Belgrade, Serbia*
[122] *VINCA Institute of Nuclear Sciences, University of Belgrade, Belgrade, Serbia*
[123] *Centro de Investigaciones Energéticas Medioambientales y Tecnológicas (CIEMAT), Madrid, Spain*
[124] *Universidad Autónoma de Madrid, Madrid, Spain*
[125] *Universidad de Oviedo, Instituto Universitario de Ciencias y Tecnologías Espaciales de Asturias (ICTEA), Oviedo, Spain*
[126] *Instituto de Física de Cantabria (IFCA), CSIC-Universidad de Cantabria, Santander, Spain*
[127] *University of Colombo, Colombo, Sri Lanka*
[128] *University of Ruhuna, Department of Physics, Matara, Sri Lanka*
[129] *CERN, European Organization for Nuclear Research, Geneva, Switzerland*
[130] *PSI Center for Neutron and Muon Sciences, Villigen, Switzerland*
[131] *ETH Zurich — Institute for Particle Physics and Astrophysics (IPA), Zurich, Switzerland*
[132] *Universität Zürich, Zurich, Switzerland*
[133] *National Central University, Chung-Li, Taiwan*
[134] *National Taiwan University (NTU), Taipei, Taiwan*
[135] *High Energy Physics Research Unit, Department of Physics, Faculty of Science, Chulalongkorn University, Bangkok, Thailand*
[136] *Tunis El Manar University, Tunis, Tunisia*
[137] *Çukurova University, Physics Department, Science and Art Faculty, Adana, Turkey*
[138] *Hacettepe University, Ankara, Turkey*
[139] *Middle East Technical University, Physics Department, Ankara, Turkey*
[140] *Bogazici University, Istanbul, Turkey*
[141] *Istanbul Technical University, Istanbul, Turkey*
[142] *Istanbul University, Istanbul, Turkey*
[143] *Yildiz Technical University, Istanbul, Turkey*
[144] *Institute for Scintillation Materials of National Academy of Science of Ukraine, Kharkiv, Ukraine*
[145] *National Science Centre, Kharkiv Institute of Physics and Technology, Kharkiv, Ukraine*
[146] *University of Bristol, Bristol, U.K.*
[147] *Rutherford Appleton Laboratory, Didcot, U.K.*

2026 JINST 21 P04002

[148] *Imperial College, London, U.K.*
[149] *Brunel University, Uxbridge, U.K.*
[150] *Baylor University, Waco, Texas, U.S.A.*
[151] *Bethel University, St. Paul, Minnesota, U.S.A.*
[152] *Catholic University of America, Washington, DC, U.S.A.*
[153] *The University of Alabama, Tuscaloosa, Alabama, U.S.A.*
[154] *Boston University, Boston, Massachusetts, U.S.A.*
[155] *Brown University, Providence, Rhode Island, U.S.A.*
[156] *University of California, Davis, Davis, California, U.S.A.*
[157] *University of California, Los Angeles, California, U.S.A.*
[158] *University of California, Riverside, Riverside, California, U.S.A.*
[159] *University of California, San Diego, La Jolla, California, U.S.A.*
[160] *University of California, Santa Barbara — Department of Physics, Santa Barbara, California, U.S.A.*
[161] *California Institute of Technology, Pasadena, California, U.S.A.*
[162] *Carnegie Mellon University, Pittsburgh, Pennsylvania, U.S.A.*
[163] *University of Colorado Boulder, Boulder, Colorado, U.S.A.*
[164] *Cornell University, Ithaca, New York, U.S.A.*
[165] *Fermi National Accelerator Laboratory, Batavia, Illinois, U.S.A.*
[166] *University of Florida, Gainesville, Florida, U.S.A.*
[167] *Florida State University, Tallahassee, Florida, U.S.A.*
[168] *Florida Institute of Technology, Melbourne, Florida, U.S.A.*
[169] *University of Illinois Chicago, Chicago, Illinois, U.S.A.*
[170] *The University of Iowa, Iowa City, Iowa, U.S.A.*
[171] *Johns Hopkins University, Baltimore, Maryland, U.S.A.*
[172] *The University of Kansas, Lawrence, Kansas, U.S.A.*
[173] *Kansas State University, Manhattan, Kansas, U.S.A.*
[174] *University of Maryland, College Park, Maryland, U.S.A.*
[175] *Massachusetts Institute of Technology, Cambridge, Massachusetts, U.S.A.*
[176] *University of Minnesota, Minneapolis, Minnesota, U.S.A.*
[177] *University of Nebraska-Lincoln, Lincoln, Nebraska, U.S.A.*
[178] *State University of New York at Buffalo, Buffalo, New York, U.S.A.*
[179] *Northeastern University, Boston, Massachusetts, U.S.A.*
[180] *Northwestern University, Evanston, Illinois, U.S.A.*
[181] *University of Notre Dame, Notre Dame, Indiana, U.S.A.*
[182] *The Ohio State University, Columbus, Ohio, U.S.A.*
[183] *Princeton University, Princeton, New Jersey, U.S.A.*
[184] *University of Puerto Rico, Mayaguez, Puerto Rico, U.S.A.*
[185] *Purdue University, West Lafayette, Indiana, U.S.A.*
[186] *Purdue University Northwest, Hammond, Indiana, U.S.A.*
[187] *Rice University, Houston, Texas, U.S.A.*
[188] *University of Rochester, Rochester, New York, U.S.A.*
[189] *Rutgers, The State University of New Jersey, Piscataway, New Jersey, U.S.A.*
[190] *University of Tennessee, Knoxville, Tennessee, U.S.A.*
[191] *Texas A&M University, College Station, Texas, U.S.A.*
[192] *Texas Tech University, Lubbock, Texas, U.S.A.*
[193] *Vanderbilt University, Nashville, Tennessee, U.S.A.*
[194] *University of Virginia, Charlottesville, Virginia, U.S.A.*
[195] *Wayne State University, Detroit, Michigan, U.S.A.*
[196] *University of Wisconsin — Madison, Madison, Wisconsin, U.S.A.*
[197] *An institute or international laboratory covered by a cooperation agreement with CERN*
[198] *An institute formerly covered by a cooperation agreement with CERN*

[a] *Also at Yerevan State University, Yerevan, Armenia*

2026 JINST 21 P04002

[b] Also at TU Wien, Vienna, Austria
[c] Also at Ghent University, Ghent, Belgium
[d] Also at FACAMP — Faculdades de Campinas, Sao Paulo, Brazil
[e] Also at Universidade Estadual de Campinas, Campinas, Brazil
[f] Also at Federal University of Rio Grande do Sul, Porto Alegre, Brazil
[g] Also at The University of the State of Amazonas, Manaus, Brazil
[h] Also at University of Chinese Academy of Sciences, Beijing, China
[i] Also at University of Chinese Academy of Sciences, Beijing, China
[j] Also at School of Physics, Zhengzhou University, Zhengzhou, China
[k] Now at Henan Normal University, Xinxiang, China
[l] Also at University of Shanghai for Science and Technology, Shanghai, China
[m] Also at The University of Iowa, Iowa City, Iowa, U.S.A.
[n] Also at Nanjing Normal University, Nanjing, China
[o] Also at Center for High Energy Physics, Peking University, Beijing, China
[p] Also at Helwan University, Cairo, Egypt
[q] Now at Zewail City of Science and Technology, Zewail, Egypt
[r] Also at Cairo University, Cairo, Egypt
[s] Also at Université de Haute Alsace, Mulhouse, France
[t] Also at Purdue University, West Lafayette, Indiana, U.S.A.
[u] Also at Another institute or international laboratory covered by a cooperation agreement with CERN
[v] Also at University of Hamburg, Hamburg, Germany
[w] Also at RWTH Aachen University, III. Physikalisches Institut A, Aachen, Germany
[x] Also at Bergische University Wuppertal (BUW), Wuppertal, Germany
[y] Also at Brandenburg University of Technology, Cottbus, Germany
[z] Also at Forschungszentrum Jülich, Juelich, Germany
[aa] Now at RWTH Aachen University, III. Physikalisches Institut A, Aachen, Germany
[ab] Also at CERN, European Organization for Nuclear Research, Geneva, Switzerland
[ac] Also at HUN-REN ATOMKI — Institute of Nuclear Research, Debrecen, Hungary
[ad] Now at Universitatea Babes-Bolyai — Facultatea de Fizica, Cluj-Napoca, Romania
[ae] Also at MTA-ELTE Lendület CMS Particle and Nuclear Physics Group, Eötvös Loránd University, Budapest, Hungary
[af] Also at HUN-REN Wigner Research Centre for Physics, Budapest, Hungary
[ag] Also at Physics Department, Faculty of Science, Assiut University, Assiut, Egypt
[ah] Also at The University of Kansas, Lawrence, Kansas, U.S.A.
[ai] Also at Punjab Agricultural University, Ludhiana, India
[aj] Also at University of Hyderabad, Hyderabad, India
[ak] Also at Indian Institute of Science (IISc), Bangalore, India
[al] Also at University of Visva-Bharati, Santiniketan, India
[am] Also at Institute of Physics, Bhubaneswar, India
[an] Also at Deutsches Elektronen-Synchrotron, Hamburg, Germany
[ao] Also at Isfahan University of Technology, Isfahan, Iran
[ap] Also at Sharif University of Technology, Tehran, Iran
[aq] Also at Department of Physics, University of Science and Technology of Mazandaran, Behshahr, Iran
[ar] Also at Department of Physics, Faculty of Science, Arak University, ARAK, Iran
[as] Also at Italian National Agency for New Technologies, Energy and Sustainable Economic Development, Bologna, Italy
[at] Also at Centro Siciliano di Fisica Nucleare e di Struttura Della Materia, Catania, Italy
[au] Also at James Madison University, Harrisonburg, N/A, U.S.A.
[av] Also at Università degli Studi Guglielmo Marconi, Roma, Italy
[aw] Also at Scuola Superiore Meridionale, Università di Napoli 'Federico II', Napoli, Italy
[ax] Also at Fermi National Accelerator Laboratory, Batavia, Illinois, U.S.A.
[ay] Also at Lulea University of Technology, Lulea, Sweden
[az] Also at Consiglio Nazionale delle Ricerche — Istituto Officina dei Materiali, Perugia, Italy
[ba] Also at UPES — University of Petroleum and Energy Studies, Dehradun, India
[bb] Also at Institut de Physique des 2 Infinis de Lyon (IP2I), Villeurbanne, France

2026 JINST 21 P04002

[bc] *Also at Department of Applied Physics, Faculty of Science and Technology, Universiti Kebangsaan Malaysia, Bangi, Malaysia*
[bd] *Also at Trincomalee Campus, Eastern University, Sri Lanka, Nilaveli, Sri Lanka*
[be] *Also at Saegis Campus, Nugegoda, Sri Lanka*
[bf] *Also at National and Kapodistrian University of Athens, Athens, Greece*
[bg] *Also at Ecole Polytechnique Fédérale Lausanne, Lausanne, Switzerland*
[bh] *Also at Universität Zürich, Zurich, Switzerland*
[bi] *Also at Stefan Meyer Institute for Subatomic Physics, Vienna, Austria*
[bj] *Also at Near East University, Research Center of Experimental Health Science, Mersin, Turkey*
[bk] *Also at Konya Technical University, Konya, Turkey*
[bl] *Also at Istanbul Topkapi University, Istanbul, Turkey*
[bm] *Also at Izmir Bakircay University, Izmir, Turkey*
[bn] *Also at Adiyaman University, Adiyaman, Turkey*
[bo] *Also at Bozok Universitetesi Rektörlügü, Yozgat, Turkey*
[bp] *Also at Istanbul Sabahattin Zaim University, Istanbul, Turkey*
[bq] *Also at Marmara University, Istanbul, Turkey*
[br] *Also at Milli Savunma University, Istanbul, Turkey*
[bs] *Also at Informatics and Information Security Research Center, Gebze/Kocaeli, Turkey*
[bt] *Also at Kafkas University, Kars, Turkey*
[bu] *Now at Istanbul Okan University, Istanbul, Turkey*
[bv] *Also at Istanbul University — Cerrahpasa, Faculty of Engineering, Istanbul, Turkey*
[bw] *Also at Istinye University, Istanbul, Turkey*
[bx] *Also at School of Physics and Astronomy, University of Southampton, Southampton, U.K.*
[by] *Also at Monash University, Faculty of Science, Clayton, Australia*
[bz] *Also at Università di Torino, Torino, Italy*
[ca] *Also at Karamanoğlu Mehmetbey University, Karaman, Turkey*
[cb] *Also at California Lutheran University;, Thousand Oaks, California, U.S.A.*
[cc] *Also at California Institute of Technology, Pasadena, California, U.S.A.*
[cd] *Also at United States Naval Academy, Annapolis, Maryland, U.S.A.*
[ce] *Also at Bingol University, Bingol, Turkey*
[cf] *Also at Georgian Technical University, Tbilisi, Georgia*
[cg] *Also at Sinop University, Sinop, Turkey*
[ch] *Also at Erciyes University, Kayseri, Turkey*
[ci] *Also at Horia Hulubei National Institute of Physics and Nuclear Engineering (IFIN-HH), Bucharest, Romania*
[cj] *Now at Another institute formerly covered by a cooperation agreement with CERN*
[ck] *Also at Another institute formerly covered by a cooperation agreement with CERN*
[cl] *Also at Hamad Bin Khalifa University (HBKU), Doha, Qatar*
[cm] *Also at Yerevan Physics Institute, Yerevan, Armenia*
[cn] *Also at Imperial College, London, U.K.*
[co] *Now at Yerevan Physics Institute, Yerevan, Armenia*
[†] *Deceased*

2026 JINST 21 P04002